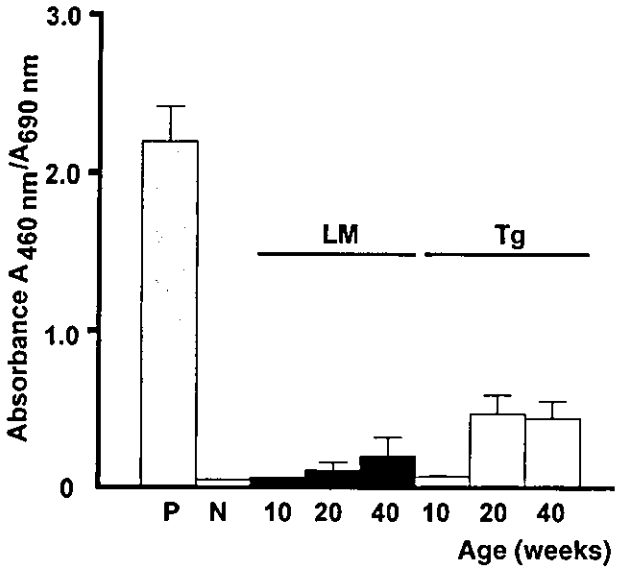

Fig. 8. Telomerase activites in pancreatic islets. Pancreatic islets were lysed in ice-cold lysis buffer and 10 μg of protein extract was subjected to the telomerase PCR ELISA assay (n=10 each). Absorbance was measured at 450 nm, with 690 nm used as a reference. MIN6 cell extract (P) and lysis buffer (N) were analysed as controls. LM, littermates; Tg, CDK4 R24C-Tg mice

[28]. Based on these observations, we concluded that insulinoma did not develop in the CDK4 R24C-Tg mice.

At 60 and 120 min after the intraperitoneal glucose injection, blood glucose concentrations increased with age in littermates. Because of an abundant food supply and hypomotility in the narrow cage, age-dependent obese mice acquired insulin resistance. Although a similar increase in body weight was observed in CDK4 R24C-Tg, their blood glucose concentrations did not increase at 60 and 120 min with age. The CDK4 R24C-Tg mice possess the ability to secrete an adequate amount of insulin in response to increased insulin demand. At 25 weeks of age, the plasma insulin concentration curve of littermates after glucose injection showed one peak at 30 min, and the concentration of insulin at 120 min was not high enough to suppress the blood glucose concentrations. Conversely, the insulin curve of CDK4 R24C-Tg mice showed two peaks, and a sufficient amount of insulin was secreted to appropriately control the blood glucose concentrations for 120 min.

Although CDK4 R24C-Tg mice demonstrated the better glucose tolerance, HbA_1c levels were not statistically different between CDK4 R24C-Tg mice and their littermates. This finding ruled out the possibility of chronic hypoglycaemia due to the constitutive excessive insulin secretion in CDK4 R24C-Tg mice. The differences in the capacity for insulin secretion could only be detected when both mice were intraperitoneally injected with 2 mg/g body weight of glucose. Blood glucose homeostasis is highly differentiated in CDK4 R24C-Tg mice such that dispensable insulin is not secreted except when glucose is loaded and a large amount of insulin is needed. It has recently been reported that levels of preproinsulin I and II mRNAs are not significantly increased in $CDK4^{R24C/R24C}$ mice, whereas there is a dramatic reduction in preproinsulin levels in $CDK4^{-/-}$ mice [29]. These results suggest that CDK4 may play a critical role not only in postnatal pancreatic development, but also in the functional maturation of insulin secretion.

Even after 18 months, no insulinoma developed in the CDK4 R24C-Tg mice. Conversely, homozygous $CDK4^{R24C/R24C}$ knock-in mice have been shown to develop multiple tumours, including endocrine tumours and haemangiosarcomas, at the age of 1 year [6]. Heterozygous $CDK4^{WT/R24C}$ knock-in mice have also been observed to develop multiple tumours [8]. Given the powerful activity of the *insulin* promoter and the many copies of the *CDK4 R24C* transgene inserted into the genome of the CDK4 R24C-Tg mice, it is unlikely that the level of transgene expression in the CDK4 R24C-Tg mice used in this study was lower than that in the knock-in mice used in previous studies. The level of CDK4 R24C expression driven by the *insulin* promoter in CDK4 R24C-Tg mice was four times higher than the level of CDK4 expression driven by the *CDK4* promoter. These data rule out the existence of a threshold of CDK4 activity for tumourigenesis and indicate that tumour development is not determined simply by the level of CDK4 R24C expression.

Studies on transgenic mice expressing CDK4 in epidermis or astrocytes have reported that CDK4 overexpression alone is not sufficient to cause tumour formation [30, 31]. The D-type cyclins control cyclin D/CDK4 activity by binding to and activating CDK4 [1]. However, it has been demonstrated that the overexpression of both cyclin D1 and CDK4 does not have a combined effect on tumour development [32, 33]. CDK4 may have other cyclin partners and additional roles to the phosphorylation of Rb. It is possible that CDK4 is regulated differently to CDK4 R24C since the amplification and overexpression of CDK4 has been observed in a wide spectrum of human tumours [34], whereas CDK4 R24C has been shown to be overexpressed only in sporadic and familial melanomas [9, 10].

The presence and the absence of neoplasms in $CDK4^{R24C/R24C}$ knock-in mice and CDK4 R24C-Tg mice respectively, suggests that the onset of CDK4 R24C expression may well govern neoplasm development. In knock-in mice with the germ line mutation, CDK4 R24C was expressed even in poorly differentiated beta cells, which could have caused beta cell transformation. The lack of malignant conversion in CDR4 R24C-Tg mice may be due to the fact that CDK4 R24C was only expressed in terminally differentiated beta cells under the control of the *insulin* promoter.

CDK4 R24C-Tg mice in an N4 backcross to C57BL/6 or DBA2 showed a significant increase in islet area compared with their littermates, and this was similar to that observed in the original CDK4 R24C-Tg mice in BDF1 background. The poor glucose tolerance of C57BL/6 mice compared with DBA2 wild-type mice was shown to be due to the genetic background of these littermates. In CDK4 R24C-Tg mice in an N4 backcross to C57BL/6 or DBA2, glucose regulation was intact and no hypoglycaemia was observed. These results indicate that the increase in islet area and the highly differentiated beta cell phenotype induced by CDK4 R24C overexpression are independent of the genetic background.

The proliferation and differentiation of beta cells are not induced concurrently, and the ability of highly differentiated beta cells to proliferate is thought to be extremely restricted. Using a genetic-lineage-marking approach, it has previously been shown that the maintenance of adult pancreatic beta cell mass in mice is not dependent on the stem cells, but on the self-duplication of pre-existing beta cells [35]. Beta cell area is determined by the balance between the rate of neogenesis or proliferation and the rate of apoptosis [36]. Levels of beta cell proliferation as assessed by 5-bromo-2′-deoxyuridine (BrdU) incorporation were 2.5 times higher in the islets of $CDK4^{R24C/R24C}$ mice than in the islets of their littermates at the age of 10 days [7]. The remarkable proliferation of beta cells observed in CDK4 R24C-Tg mice in our study demonstrated that beta cells could proliferate even at 25 weeks of age (i.e. at the highly differentiated stage) when the *insulin* promoter is functioning.

In this paper we have demonstrated in our transgenic mouse model that pancreatic islet beta cells proliferate significantly, with the preservation of highly differentiated phenotypes, irrespective of the genetic background. Based on this evidence, the postnatal activation of CDK4 in pancreatic islets may potentially be used for the therapeutic stimulation of proliferation of differentiated pancreatic islet beta cells. Human pancreatic islets transduced with CDK4 R24C by lentivirus show proliferative potential in response to glucose stimulation in vitro [37]. The postnatal activation of CDK4 through the use of new techniques (including the administration of vectors expressing *CDK4 R24C* under the control of the *insulin* promoter or CDK4-activating drugs) could potentially lead to the postnatal proliferation of pancreatic islet beta cells without neoplasm formation, thus providing a radical new treatment for diabetes.

Acknowledgements. This study was supported by a Grant-in-Aid for Scientific Research from Japanese Society for the Promotion of Science and a Cooperative Link of Unique Science and Technology for Economic Revitalization (CLUSTER). The authors are not aware of any conflicts of interest.

References

1. Sherr CJ (1996) Cancer cell cycle. Science 274:1672–1677
2. Kitagawa M, Higashi H, Jung HK et al. (1996) The consensus motif for phosphorylation by cyclin D1-Cdk4 is different from that for phosphorylation by cyclin A/E-Cdk2. EMBO J 15:7060–7069
3. Sherr CJ, Roberts JM (1999) CDK inhibitors: positive and negative regulators of G_1-phase progression. Genes Dev 13:1501–1512
4. Yamaoka T, Itakura M (1999) Development of pancreatic islets. Int J Mol Med 3:247–261
5. Tsutsui T, Hesabi B, Moons DS et al. (1999) Targeted disruption of CDK4 delays cell entry with enhanced $p27^{Kip1}$ activity. Mol Cell Biol 10:7011–7019
6. Rane SG, Dubus P, Mettus RV et al. (1999) Loss of CDK4 expression causes insulin-deficient diabetes and Cdk4 activation results in beta-islet cell hyperplasia. Nat Genet 22:44–52
7. Martin J, Hunt SL, Dudus P et al. (2003) Genetic rescue of Cdk4 *null* mice restores pancreatic beta-cell proliferation but not homeostatic cell number. Oncogene 22:5261–5269
8. Sotillo R, Dubus P, Martin J et al. (2001) Wide spectrum of tumors in knock-in mice carrying a Cdk4 protein insensitive to INK4 inhibitors. EMBO J 20:6637–6647
9. Wolfel T, Hauer M, Schneider J et al. (1995) A $p16^{INK4a}$-insensitive CDK4 mutant targeted by cytolytic T lymphocytes in a human melanoma. Science 269:1281–1284
10. Zou L, Weger J, Yang Q et al. (1996) Germline mutations in the $p16^{INK4a}$ binding domain of CDK4 in familial melanoma. Nat Genet 12:97–99
11. Yamaoka T, Idehara C, Yano M et al. (1998) Hypoplasia of pancreatic islets in transgenic mice expressing activin receptor mutants. J Clin Invest 102:294–301
12. Hogan B, Beddington R, Costantini F, Lacy E (1994) Manipulating the mouse embryo. A laboratory manual, 2nd edition. Cold Spring Harbor Laboratory Press, New York
13. Moritani M, Yoshimoto K, Ii S et al. (1996) Prevention of adoptively transferred diabetes in nonobese diabetic mice with IL-10-transduced islet-specific Th1 lymphocytes. J Clin Invest 98:1851–1859
14. Gotoh M, Maki T, Kiyoizumi T, Satomo S, Monaco AP (1985) An improved method for isolation of mouse pancreatic islets. Transplantation 40:437–438
15. Kato A, Takahashi H, Takahashi Y, Matsushime H (1997) Inactivation of the cyclin D-dependent kinase in the rat fibroblast cell line, 3Y1, induced by contact inhibition. J Biol Chem 272:8065–8070
16. Matsushime H, Ewen ME, Strom DK et al. (1992) Identification and properties of an atypical catalytic subunit ($p34^{PSK-J3}$/cdk4) for mammalian D type G1 cyclins. Cell 71:323–334
17. Yamada T, Brunstedt J, Solomon T (1983) Chronic effects of caerulein and secretion on endocrine of the rat. Am J Physiol 24:G541–G545
18. Kim NW, Piatyszek MA, Prowse KR et al. (1994) Specific association of human telomerase activity with immortal cells and cancer. Science 266:2011–2015
19. Asplund K (1973) Dynamics of insulin release from the fetal and neonatal rat pancreas. Eur J Clin Invest 3:338–344
20. Hole RL, Pian-Smith MC, Sharp GW (1988) Development of the biphasic response to glucose in fetal and neonatal rat pancreas. Am J Physiol 254:E167–E174
21. Otonkoski T, Anderson S, Knip M, Simell O (1988) Maturation of insulin response to glucose during human fetal and neonatal development. Diabetes 37:286–291

22. Weinhaus AF, Poronnik P, Cook DI, Tuch BE (1995) Insulin secretagogues, but not glucose, stimulate an increase in [Ca++] in the fetal rat beta cell. Diabetes 44:118–124
23. Boden G, Murer E, Mozzoli M (1994) Glucose transporter proteins in human insulinoma. Ann Intern Med 121:109–112
24. Miyamoto T, Kakizawa T, Ichikawa K, Nishio, S, Kajikawa S, Hashizume K (2001) Expression of dominant negative form of PAX4 in human insulinoma. Biochem Biophys Res Commun 282:34–40
25. Pavelic K, Hrascan R, Kapitanovic S et al. (1995) Multiple genetic alterations in malignant metastatic insulinomas. J Pathol 177:395–400
26. Pavelic K, Hrascan R, Kapitanovic S et al. (1996) Molecular genetics of malignant insulinoma. Anticancer Res 16:1707–1717
27. Rheinwald JG, Hahn WC, Ramsey MR et al. (2002) A two-stage, $p16^{INK4a}$- and p53-dependent keratinocyte senescence mechanism that limits replicative potential independent of telomere status. Mol Cell Biol 22:5157–5172
28. Fowler DL, Wood WG, Koontz PG Jr (1980) Endogenous hyperinsulinism. Am J Gastroenterol 74:321–327
29. Mettus RV, Rane SG (2003) Characterization of the abnormal pancreatic development, reduced growth and infertility in Cdk4 mutant mice. Oncogene 22:8413–8421
30. Miliani de Marval PL, Gimenez-Conti IB, LaCave M, Martinez LA, Conti CJ, Rodriguez-Puebla ML (2001) Transgenic expression of cyclin-dependent kinase 4 results in epidermal hyperplasia, hypertrophy, and severe dermal fibrosis. Am J Pathol 159:369–379
31. Huang ZY, Baldwin RL, Hedrick NM, Gutmann DH (2002) Astrocyte-specific expression of CDK4 is not sufficient for tumor formation, but cooperates with p53 heterozygosity to provide a growth advantage for astrocytes in vivo. Oncogene 21:1325–1334
32. Miliani de Marval PL, Macias E, Conti CJ, Rodriguez-Puebla ML (2004) Enhanced malignant tumorigenesis in Cdk4 transgenic mice. Oncogene 23:1863–1873
33. Lazarov M, Kubo Y, Cai T et al. (2002) CDK4 coexpression with Ras generates malignant human epidermal tumorigenesis. Nat Med 8:1105–1114
34. Ortega S, Malumbres M, Barbacid M (2002) Cyclin D-dependent kinases, INK4 inhibitors and cancer. Biochim Biophys Acta 1602:73–87
35. Dor Y, Brown J, Martinez OI, Melton DA (2004) Adult pancreatic beta-cells are formed by self-duplication rather than stem-cell differentiation. Nature 429:41–46
36. Bonner-Weir S (2000) Life and death of the pancreatic beta cells. Trends Endocrinol Metab 11:375–78
37. Marzo N, Mora C, Fabregat ME et al. (2004) Pancreatic islets from cyclin-dependent kinase 4/R24C (Cdk4) knockin mice have significantly increased beta cell mass and are physiologically functional, indicating that Cdk4 is a potential target for pancreatic beta cell mass regeneration in Type 1 diabetes. Diabetologia 47:686–694

Modern Pathology (2004) 17, 423–429

www.modernpathology.org

Diagnostic importance of CD179a/b as markers of precursor B-cell lymphoblastic lymphoma

Nobutaka Kiyokawa[1], Takaomi Sekino[1], Tsubasa Matsui[1], Hisami Takenouchi[1], Kenichi Mimori[1], Wei-ran Tang[1], Jun Matsui[1], Tomoko Taguchi[1], Yohko U Katagiri[1], Hajime Okita[1], Yoshinobu Matsuo[2], Hajime Karasuyama[3] and Junichiro Fujimoto[1]

[1]*Department of Developmental Biology, National Research Institute for Child Health and Development, Japan;* [2]*Fujisaki Cell Center, Hayashibara Biochemical Labs Inc, Okayama, Japan and* [3]*Department of Immune Regulation, Tokyo Medical and Dental University, Graduate School of Medicine, Tokyo, Japan*

Surrogate light chains consisting of VpreB (CD179a) and λ5 (CD179b) are expressed in precursor B cells lacking a complete form of immunoglobulin and are thought to act as substitutes for conventional light chains. Upon differentiation to immature and mature B cells, CD179a/b disappear and are replaced with conventional light chains. Thus, these molecules may be useful as essential markers of precursor B cells. To examine the expression of the surrogate light-chain components CD179a and CD179b in precursor B-cell lymphoblastic lymphoma, we analyzed tissue sections using immunohistochemistry techniques. Among a number of monoclonal antibodies for the surrogate light chains, VpreB8 and SL11 were found to detect CD179a and CD179b, respectively, in acetone-fixed fresh frozen sections. Moreover, we also observed VpreB8 staining in formalin-fixed, paraffin-embedded sections. Using these antibodies, we found that CD179a/b were specifically expressed in precursor B-cell lymphoblastic lymphomas, but not in mature B-cell lymphomas in childhood. Furthermore, other pediatric tumors that must be included in a differential diagnosis of precursor B-cell lymphoblastic lymphoma, including precursor T-cell lymphoblastic lymphoma, extramedullary myeloid tumors, and Ewing sarcoma, were also negative for both CD179a and CD179b. Our data indicate that CD179a and CD179b may be important markers for the immunophenotypic diagnosis of precursor B-cell lymphoblastic lymphomas.
Modern Pathology (2004) **17**, 423–429, advance online publication, 20 February 2004; doi:10.1038/modpathol.3800079

Keywords: CD179a/b; lymphoblastic lymphoma; precursor B cells; immunohistochemistry; diagnosis

B cells are characterized by the surface expression of immunoglobulin (Ig), consisting of a heavy chain (HC) and conventional κ or λ light chains (LCs). The expressed in B cells is associated with the Igα/Igβ (CD79a/b) complex and forms a B-cell antigen receptor complex. In contrast to these mature B cells, precursor B cells do not express Ig, although they do contain Ig-related components. For example, more primitive pro-B cells already express the Igα/Igβ complex and contain surrogate LCs, consisting of VpreB (CD179a) and λ5 (CD179b).[1–5] Through the successful rearrangement of HC genes, pro-B cells undergo differentiation into pre-B cells and start to express a premature antigen receptor, namely the pre-B-cell receptor (pre-BCR), consisting of μ HC, CD179a/b and the Igα/Igβ heterodimer.[6–9] Upon further differentiation from pre-B cells to B cells, CD179a/b disappear and are replaced with conventional LC.

The stage-specific developmental expression of Ig-related molecules is an essential characteristic of B-lineage cells and is conserved not only in normal cells but also in neoplastic cells of B lineage. Indeed, precursor B acute lymphoblastic leukemias (ALL), which originate from precursor B cells and lack the complete form of Ig, are known to express CD179a/b, while mature and Ig-expressing B-cell ALLs do not.[10] Precursor B-cell lymphoblastic lymphoma (B-LBL) is a disease in which neoplastic precursor B cells proliferate without the obvious involvement of blood or bone marrow and thus exhibits immunophenotypic characteristics that are similar to those of precursor B-ALL.[11,12] Neoplasms of precursor B cells most commonly present as a form of ALL during childhood, and the presentation of B-LBL is infrequent, but may occur in patients of any

Correspondence: N Kiyokawa, MD, PhD, Department of Developmental Biology, National Research Institute for Child Health and Development, 3-35-31, Taishido, Setagaya-ku, Tokyo 154-8567, Japan.
E-mail: nkiyokawa@nch.go.jp
Received 21 August 2003; revised 26 November 2003; accepted 26 December 2003; published online 20 February 2004

age, frequently involving the skin, bone, or lymph nodes. Owing to the rareness of B-LBL and its morphological and immunophenotypic similarities to mature B-cell lymphomas in some cases, distinguishing between these diseases is of great importance, especially in the field of pediatric oncology, because the treatment strategies for these two diseases are quite different. In addition, other tumors, including precursor T-cell lymphoblastic lymphoma (T-LBL), extramedullary myeloid tumors, and Ewing sarcoma, must also be included in a differential diagnosis of B-LBL.

In an attempt to characterize B-LBL using the expression of Ig-related molecules and to examine the utility of such a method for diagnosis, we examined CD179a/b expression in B-LBL tissues using immunohistochemistry. CD179a/b was found to be specifically expressed in B-LBL, but not in mature B-cell lymphomas and other tumors in childhood. The usefulness of CD179a/b as diagnostic markers for B-LBL is discussed.

Materials and methods

Materials

The human pre-B-cell line HPB-NULL[10] and the Burkitt cell line Ramos (Japanese Cancer Research Resources Bank, Tokyo, Japan) were used in this study. Cells were maintained in RPMI1640 supplemented with 10% fetal calf serum at 37°C in a humidified 5% CO_2 atmosphere.

Biopsy specimens from pediatric patients, including 11 patients with B-LBL, seven patients with Burkitt lymphoma, three patients with diffuse large B-cell lymphoma, seven patients with T-LBL, three patients with extramedullary myeloid tumors, and three patients with Ewing sarcoma, were selected from medical files collected between 1985 and 2003 at the Department of Developmental Biology, National Research Institute for Child Health and Development. In each case, the initial diagnosis was based on morphological observations of hematoxylin and eosin (H&E)-stained, formalin-fixed, paraffin-embedded tissues, the immunophenotypic characteristics revealed by immunohistochemistry using acetone-fixed, fresh frozen sections, and the patient's clinical features. In some cases, immunophenotyping was also performed using flow cytometric analysis of a single-cell suspension prepared from the tissue. To examine CD179a/b expression, snap-frozen tissues in OCT compounds stored at −85°C after the initial diagnosis were used.

The following mouse monoclonal antibodies (mAbs) were used in this study: anti-CD179a (HSL96), anti-CD179b (HSL11), anti-conformational pre-BCR (HSL2),[10] anti-CD20 (L26),[13] anti-HLA-DR,[14] and anti-CD10 (IF6).[15] HSL2 is a unique mAb that does not bind to each component of the pre-BCR, but recognizes a conformational epitope formed only when the μ HC and CD179a/b surrogate LC associate with each other to make the pre-BCR complex.[10] In addition, several commercially available mAbs were also used: anti-μ (G20-127), anti-CD179a (VpreB8 and VpreB9), and anti-CD19 (Leu12) from BD Pharmingen (San Diego, CA, USA); anti-κ (HP6053) and anti-λ (HP6054) from Zymed Laboratories Inc. (San Francisco, CA, USA); anti-CD79a (HM-57), anti-CD22 (4KB128), and anti-TdT (HT-1/3/4) from DAKO (Glostrup, Denmark); anti-CD179a (4G7) from Coulter/Immunotech Inc. (Westbrook, MA, USA); anti-TdT (SEN28) from Nichirei Co. (Tokyo, Japan); and anti-CD179a (B-MAD-688) from Biocarta (San Diego, CA, USA). The anti-CD77 (1A4) used in this study was a generous gift from Dr S Hakomori of the University of Washington, Seattle, WA, USA and Otsuka Assay Laboratories, Kawauchi-cho, Tokushima, Japan. Secondary Abs, including fluorescence- and enzyme-conjugated Abs, were purchased from Jackson Laboratory, Inc., West Grove, PA, USA.

Flow Cytometry

The cells were stained with mAbs and analyzed by flow cytometry (EPICS-XL, Coulter) as described previously.[15] Cytoplasmic antigens were stained using CytoStain™ Kits (BD Pharmingen), according to the manufacturer's protocol.

Immunohistochemistry

Immunohistochemical staining of acetone-fixed fresh frozen sections was performed as described elsewhere.[16] Briefly, fresh frozen sections from each tissue were prepared using a cryostat apparatus and fixed in acetone for 15 min at 4°C. After washing in phosphate-buffered saline (PBS) and blocking with normal rabbit serum, the sections were incubated with mAbs at appropriate dilutions for 30 min at room temperature. Sections were then washed with PBS and incubated with horseradish peroxidase (HRP)-conjugated rabbit anti-mouse antibodies for 30 min at room temperature. After washing with PBS, color development was performed in diaminobenzidine solution (10 mM in 0.05 M Tris-HCl, pH 7.5) with 0.003% H_2O_2.

For the cell line samples, the cells were cytocentrifuged on slide glasses using Cytospin III (Shandon Scientific Ltd., Pittsburgh, PA, USA). After fixation with acetone, immunohistochemical staining was performed as described above. In addition, other fixatives, including paraformaldehyde and Zamboni's fixative, were also tested.

The formalin-fixed, paraffin-embedded tissue specimens were initially deparaffinized and then treated using the heat-induced epitope retrieval method in 10 mM of citrate buffer, pH 6.0; immunohistochemical staining was performed using the CSA system (DAKO) according to the manufacturer's protocol.

Results

Immunohistochemical Staining of CD179a/b in Acetone-fixed Cytocentrifuged Cell Lines

As reported previously and presented in Figure 1, the mAbs HSL96, HSL11, and HSL2 recognized CD179a/VpreB, CD179b/λ5, and conformational pre-BCR, respectively, in membrane-permeabilized cells when analyzed using flow cytometry.[10] We first examined whether these mAbs could also be used for immunohistochemical staining in acetone-fixed cells. When acetone-fixed, cytocentrifuged pre-B-ALL HPB-NULL cells expressing conformational pre-BCR were tested, the HSL11 mAb was able to detect CD179b at a concentration of 5 μg/ml; neither the HSL96 nor the HSL2 mAbs detected this molecule (Figure 1). Typically, a cytoplasmic staining pattern was observed in HPB-NULL cells using HSL11. In contrast, HSL11 did not react with similarly treated Ramos Burkitt cells, which express the complete form of Ig (μλ), but lack the surrogate LCs, suggesting that CD179b binds specifically to SL11.

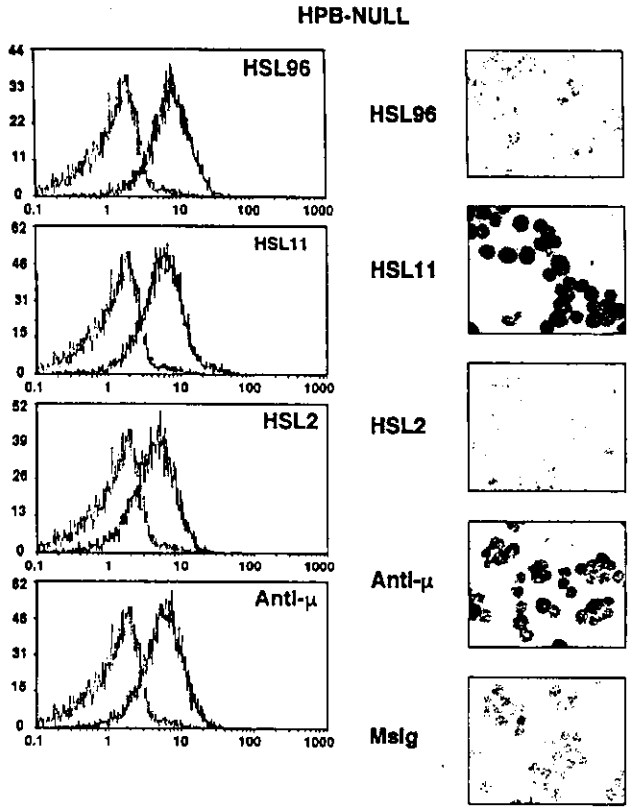

Figure 1 Immunohistochemical detection of CD179b by HSL11 in acetone-fixed, cytocentrifuged precursor B-ALL cell lines. Pre-BCR-expressing HPB-NULL cells were permeabilized and stained with specific mAbs, as indicated, and analyzed using flow cytometry (left panels). The resulting histograms (solid lines) were superimposed on those of the negative control (cells stained with isotype-matched control mouse Ig, broken light lines) and displayed. *X*-axis, fluorescence intensity; *Y*-axis, relative cell number. In parallel, HPB-NULL cells were cytocentrifuged, acetone-fixed, and stained with each mAb, as indicated, using immunohistostaining (right panels). HSL11 is strongly positive and anti-μ is moderately positive, but others are negative. MsIg, iso-type matched control mouse immunoglobulin.

We also examined the staining patterns produced by commercially available anti-CD179a mAbs: VpreB8, VpreB9, 4G7, and B-MAD-688. When these four anti-CD179a mAbs were examined, only the VpreB8 mAb reacted with CD179a in acetone-fixed HPB-NULL cells (data not shown). However, VpreB8 mAb exhibited a weak nonspecific binding with the nuclei of acetone-fixed Ramos cells at high mAb concentrations. A concentration of 1.25 μg/ml was optimized as a sufficient and specific condition for CD179a detection in precursor B-ALL cells, which does not produce a nonspecific reaction in Burkitt cells (data not shown).

We further examined whether SL11 and VpreB8 could be used for immunohistochemical staining in cells treated with other fixatives and observed that both mAbs react with Zamboni's fixative-treated cells, but not with paraformaldehyde-treated cells (data not shown).

Immunohistochemical Staining of CD179a/b in Acetone-fixed Fresh Frozen Tissues

Next, we used immunohistochemistry to examine whether VpreB8 and HSL11 could detect CD179a/b in clinical childhood B-LBL specimens. When acetone-fixed fresh frozen sections prepared from biopsy specimens obtained from B-LBL patients were examined using immunohistochemical staining, both VpreB8 and HSL11 were found to react with the tissues (Figure 2 and Table 1). Typically, a diffuse cytoplasmic staining pattern was observed in B-LBL tissues using both mAbs (Figure 2). Cases were considered as positive if most of the blasts present in the tissue were clearly stained. As summarized in Table 1, nine out of 10 (90%) B-LBL patients and eight out of 11 (73%) B-LBL patients were positive for VpreB8 and HSL11, respectively. In contrast, no positive staining for VpreB8 or HSL11 was seen in either the Burkitt lymphoma tissues (seven cases) or the diffuse large B-cell lymphoma tissues (three cases), suggesting that both VpreB8 and HSL11 react specifically with B-LBL cells, but not with mature B-cell lymphomas in childhood.

We also examined the other pediatric tumors that must also be included in a differential diagnosis of B-LBL. As presented in Table 2, when acetone-fixed fresh frozen sections prepared from biopsy specimens obtained from seven T-LBL cases, three extramedullary myeloid tumors, and two Ewing sarcoma cases were examined similarly, all of these cases were negative for both VpreB8 and HSL11, indicating the specificity of these mAbs to B-LBL cells.

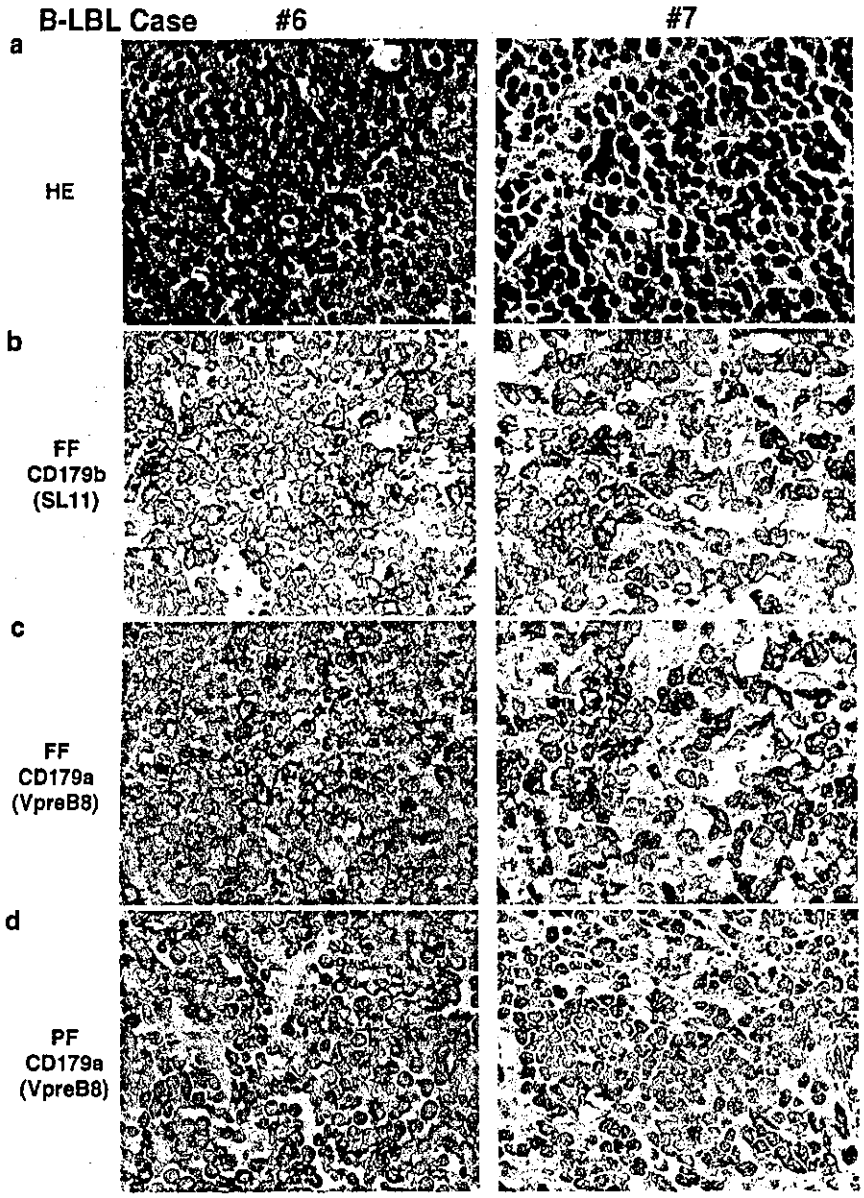

Figure 2 Immunohistochemical detection of CD179a and CD179b. CD179a and CD179b were detected in B-lymphoblastic lymphoma tissues using immunohistochemical staining on acetone-fixed fresh frozen sections ((b), (c), FF) and formalin-fixed, paraffin-embedded tissue sections ((d), PF) from biopsy tissues. The H&E-staining of formalin-fixed and paraffin-embdded tissues is also shown ((a), HE).

Immunohistochemical Staining of CD179a in Formalin-fixed, Paraffin-embedded Tissues

Next, we examined whether mAbs against CD179a and CD179b could be used in formalin-fixed, paraffin-embedded tissues. When paraffin-embedded tissues prepared from clinical specimens obtained from B-LBL patients were examined using immunohistochemical staining with the heat-induced epitope retrieval treatment, only VpreB8 reacted with the tissue. The staining results were consistent with those obtained from the immunostaining of acetone-fixed frozen sections. None of the other mAbs reacted with the B-LBL samples. Since higher concentrations of VpreB8 resulted in nonspecific nuclear staining in paraffin sections of Burkitt lymphomas, care must be taken when deciding the appropriate conditions for the use of this mAb.

Discussion

In the current study, we clearly presented that both VpreB8 and HSL11 are useful for the immunohistochemical detection of CD179a and CD179b, respectively, in acetone-fixed B-LBL tissues. Furthermore, VpreB8 can also be used in paraffin-embedded sections. The reactivities of these Abs were highly specific for B-LBL. Reactivity was not seen in tissues of Burkitt lymphoma, diffuse large B-cell

Table 1 Detection of CD179a and CD179b in B-lineage lymphoma tissues using immunohistochemical staining in acetone-fixed fresh frozen sections

Case no.	Age (years)	Sex	Origin	CD179a	CD179b	TdT	CD34	CD19	CD79a	DR	CD20	μ	LC	CD10	CD77
B-LBL															
1	4	M	Bil-CL	+	+	+	−	+	+	+	+P	−	−	+	−
2[a]	9	M	R-testis	+	+	+	−	+	+	+	+M	NT	NT	+	−
3	7	M	L-CL	+	+	+	−	+	+	+	−	+	−	+	−
4	5	F	L-CL	+	+	+	−	+	+	+	−	−	−	+	−
5	7	F	L-CL	+	+	+	+	+	+	+	−	+	−	+	−
6	1	F	R-CL	+	+	+	−	+	+	+	−	−	−	+	−
7	12	M	AT	+	+	−	−	+	+	+	−	−	−	+	−
8	5	F	L-upper arm	+	−	−	−	+	+	+	+M	−	−	+	NT
9	7	M	L-CL	−	−	+	−	+	+	+	+P	−	−	+	NT
10	4	F	R-radius	+	−	−	+	+	+	+	−	−	−	+	−
11	9	M	CNS	NT	+	+	NT	+	+	NT	NT	+	NT	NT	NT
Burkitt															
1	6	F	AT	−	−	−	−	+	+	+	+	+	−	−	+
2	7	M	AT	−	−	−	−	+	+	+	+	+	Lamda	+	+
3	15	M	AT	−	−	−	−	+	+	+	+	+	Lamda	+	+
4	4	M	AT	−	−	−	−	+	+	+	+	+	Kappa	+	+
5	6	M	AT	−	−	−	−	+	+	+	+	+	Kappa	+	−
6	5	M	AT	−	−	−	−	+	+	+	+	+	Kappa	+	+
7	4	M	AT	−	−	−	−	+	+	+	+	+	Lamda	+	+
B-DL															
1	7	F	R-CL	−	−	−	−	+	+	+	+	+	Lamda	−	−
2	6	M	AT	−	−	−	−	+	+	+	+	+	Lamda	−	−
3	8	M	R-CL	−	−	−	−	+	+	+	+	+	Lamda	+	−

B-LBL, precursor B-cell lymphoblastic lymphoma; DL, diffuse large cell lymphoma; Bil, bilateral; L, left; R, right; CL, cervical lymph nodes; AT, abdominal tumor; LC, light chains; NT, not tested; P, patchy staining pattern; M, membranous staining pattern.
[a]Testicular relapse of precursor B acute lymphoblastic leukemia.

Table 2 Immunohistochemical staining of CD179a and CD179b on acetone-fixed fresh frozen sections of non-B-cell lineage neoplasm tissues

	Positivity	
	CD179a	CD179b
T-LBL	0/7	0/7
Extramedullary myeloid tumors		
Granulocytic sarcoma	0/2	0/2
AMoL, skin infiltration	0/1	0/1
Ewing sarcoma	0/2	0/2

T-LBL, precursor T-cell lymphoblastic lymphoma; AMoL, acute monocytic leukemia.

lymphoma, T-LBL, extramedullary myeloid tumors, and Ewing sarcoma.

In pediatrics, the three major types of B-cell lymphoma are B-LBL, Burkitt lymphoma, and diffuse large B-cell lymphoma; the latter two types must be distinguished from B-LBL since the therapeutic protocols for these diseases are quite different from that for B-LBL. In the Berlin Frankfurt Munster (BFM) study group, for example, B-LBL cases were treated using ALL-type protocol with a total therapy duration of at least 24 months.[17] In contrast, mature B-cell lymphoma cases, including Burkitt lymphoma and diffuse large B-cell lymphoma, are treated using a short course of treatment that is usually completed within a year.[18] Each type of B-lineage lymphoma is morphologically unique and distinctive upon histological examination. In the practical pathological diagnosis of lymphomas, however, pathologists may experience difficulties in differentiating B-LBL from other B-lineage lymphomas, especially when only poor-quality biopsy specimens are available.[12] Unfortunately, pathologists are not always familiar with B-LBL because of its rarity among childhood lymphomas; as a result, patients with B-LBL may be misdiagnosed as having mature B-cell lymphoma, such as Burkitt lymphoma. The similarity in marker expression patterns for B-LBL and Burkitt lymphoma is also partly responsible for the risk of misdiagnosis.[11,12]

TdT is considered to be a reliable marker for the diagnosis of cases of precursor lymphocyte origin,[11,12] but TdT is not always positive in B-LBL cases as reported by several different groups.[19–22] For example, Mertelsmann *et al*[20] reported that TdT was absent in approximately 5% of ALL and LBL cases. Orazi *et al*[21] also reported that 6% (two out of 35) of LBL cases was TdT-negative assessed by immunohistochemical staining. On the other hand, CD34 is expressed on human bone marrow progenitor cells and leukemic blasts, and is considered to be an immature marker. Although the expression of CD34 on B-lineage lymphomas suggests their precursor B-cell origin, the positivity of CD34 among the B-LBL cases is approximately 50%. In addition, both TdT

and CD34 are not restricted to the precursor of B cells. In contrast, CD20 is a B-cell-specific marker and its expression increases with B-cell maturation. Therefore, the absence of CD20 expression in B-lineage lymphomas suggests their precursor B-cell origin. However, CD20 expression is variable among cases of B-LBL and approximately 50% of B-LBL cases are CD20-positive, exhibiting sometimes a strong membranous staining pattern.[11] Therefore, it is difficult to specify a B-precursor origin using CD20 expression alone. Based on the above evidences, the development of other markers capable of revealing a precursor B-cell origin is urgently required; in this regard, the results described here are expected to assist in the proper diagnosis of B-LBL among B-cell lymphomas in childhood.

CD179a and CD179b are essential for the development of precursor B cells. Although their biological significance is not fully understood, they are believed to serve as surrogate LCs expressed with μ HCs in pre-BCR to determine whether the clone should survive or die. After subsequent rearrangements in κ or λ LC genes, the expression of the surrogate LCs is suppressed.[6–9] The utilization of such functional molecules in the diagnosis of precursor B-cell lymphomas is appropriate if the expression is conserved even in tumor cells. In precursor B-ALL cells, we previously reported that CD179a, CD179b, and the complete form of pre-BCR were detected by HSL96, HSL11, and HSL2, respectively, and were expressed in most of the CD10-positive precursor B-ALL cases,[10] suggesting that these markers may be useful for the further classification of this disease. Consistent with this observation, CD179a and CD179b, detected by VpreB8 and HSL11, respectively, were frequently expressed in B-LBL cases, whose origin is comparable to that of precursor B-ALL. Thus, the successful employment of these functional molecules in the diagnosis of B-cell lymphomas is another important aspect emphasized in this study.

As shown here, CD179a and CD179b immunohistochemistry can identify more than 90% of B-LBL cases. In our series, the positivity of TdT among the B-LBL cases examined was lower (73%) than that of previous reports.[19–22] The reason for this discrepancy is not known, but it is noteworthy that three TdT-negative cases were positive for either CD179a or CD179b or both. Thus, by combining the TdT and CD179 markers, we believe that virtually all B-LBL cases can be properly judged as having a precursor B-cell origin. The absence of CD179a/b reactivity in Burkitt and diffuse large B-cell-type lymphomas further supports the reliability of this marker.

Occasionally, B-LBL may be misdiagnosed as Ewing sarcoma, since these two diseases have similar morphologies and immunostaining patterns.[23] CD99 (MIC2) was previously considered to be a specific marker for Ewing sarcoma, but this molecule has now been shown to be frequently expressed in B-LBL. Bone tumors with a blastic morphology and a CD45−, CD20−, MIC2+ phenotype can be diagnosed as Ewing sarcoma. In such cases, immunostaining for CD179a/b along with TdT and CD79a will lead to a proper diagnosis. In addition, immunostaining for CD179a/b is also useful for distinguishing B-LBL from either T-LBL or extramedullary myeloid tumors, both of which are included in frequent differential for B-LBL.

Diagnostic markers must be usable in paraffin sections for practical diagnostic procedures. In this regard, the utilization of mAb VpreB8 in paraffin sections, as demonstrated in this report, should facilitate its use in daily diagnostics. Caution must be exercised, however, when using VpreB8 because this antibody may produce nonspecific binding. After careful examination, we selected a concentration of 1.25 μg/ml for our system; however, this value should be evaluated for each laboratory in which the mAb is used, since differences in detection systems may affect the results. Other than VpreB8, unfortunately, none of the mAbs against CD179a/b tested in this study was useful for immunohistochemical detection in paraffin-embedded sections. Since the expression of CD179b was always accompanied by that of CD179a in our cases assessed using fresh frozen section staining (Table 1), paraffin section staining with VpreB8 may be sufficient for the diagnosis of B-LBL. However, the generation of novel mAbs against CD179a/b and preBCR that can react in paraffin sections would be useful and may provide more convincing results.

In conclusion, we have demonstrated that mAbs against CD179a/b specifically detect B-LBL tissues. Although an examination of a larger number of lymphoma tissues is required to confirm their reliability, the application of these mAbs in the immunohistochemical examination of lymphoma tissues should contribute to a precise diagnosis of B-lineage lymphomas.

Acknowledgements

This work was supported in part by Health and Labour Sciences Research Grants from the Ministry of Health, Labour and Welfare of Japan and MEXT, KAKENHI 15019129, JSPS, KAKENHI 15390133 and 15590361. This work was also supported by a grant from the Japan Health Sciences Foundation for Research on Health Sciences Focusing on Drug Innovation. Additional support was provided by a grant from Sankyo Foundation of Life Science.

We thank M Sone and S Yamauchi for their excellent secretarial works. We also thank Dr S Hakomori (Washington University) and Otsuka Assay Laboratories for gifting CD77 mAb 1A4.

References

1 Sakaguchi N, Melchers F. λ5, a new light-chain-related locus selectively expressed in pre-B lymphocytes. Nature 1986;324:579–582.
2 Kudo A, Melchers F. A second gene, VpreB in the λ5 locus of the mouse, which appears to be selectively expressed in pre-B lymphocytes. EMBO J 1987;6: 2267–2272.
3 Bauer SR, Kudo A, Melchers F. Structure and pre-B lymphocyte restricted expression of the VpreB in humans and conservation of its structure in other mammalian species. EMBO J 1988;7:111–116.
4 Hollis GF, Evans RJ, Stafford-Hollis JM, *et al.* Immunoglobulin λ light-chain-related genes 14.1 and 16.1 are expressed in pre-B cells and may encode the human immunoglobulin ω light-chain protein. Proc Natl Acad Sci USA 1989;86:5552–5556.
5 Schiff C, Bensmanna M, Gulglielmi P, *et al.* The immunoglobulin λ-like gene cluster (14.1, 16.1 and Fl1) contains gene(s) selectively expressed in pre-B cells and is the human counterpart of the mouse λ5 gene. Int Immunol 1990;2:201–207.
6 Karasuyama H, Kudo A, Melchers F. The proteins encoded by the VpreB and λ5 pre-B cell specific genes can associate with each other and with μ heavy chain. J Exp Med 1990;172:969–972.
7 Tsubata T, Reth M. The products of pre-B cell-specific genes (λ5 and VpreB) and the immunoglobulin μ chain form a complex that is transported onto the cell surface. J Exp Med 1990;172:973–976.
8 Karasuyama H, Rolink A, Shinkai Y, *et al.* The expression of VpreB/λ5 surrogate light chain in early bone marrow precursor B cells of normal and B cell-deficient mutant mice. Cell 1994;77:133–143.
9 Lassoued K, Nunez CA, Billips L, *et al.* Expression of surrogate light chain receptors is restricted to a late stage in pre-B cell differentiation. Cell 1993;73:73–86.
10 Tsuganezawa K, Kiyokawa N, Matsuo M, *et al.* Flow cytometric diagnosis of the cell lineage and developmental stage of acute lymphoblastic leukemia by novel monoclonal antibodies specific to human preB cell receptor. Blood 1998;92:4317–4324.
11 Brunning RD, Borowitz M, Matutes E, *et al.* Precursor B lymphoblastic leukaemia/lymphoblastic lymphoma (precursor B-cell acute lymphoblastic leukaemia). In: Jaffe ES, Harris NL, Stein H, Vardiman JW (eds). Pathology & Genetics: Tumours of Haematopoietic and Lymphoid Tissues. IARC Press: Lyon, 2001, pp 111–114.
12 Gatter K, Delsol G. B-cell lymphoblastic lymphoma. In: Gatter K, Delsol G (eds). The Diagnosis of Lymphoproliferative Diseases. Oxford University Press: Oxford, 2002, pp 59–63.
13 Ishii Y, Takami T, Yuasa H, *et al.* Two distinct antigen systems in human B lymphocytes: identification of cell surface and intracellular antigens using monoclonal antibody. Clin Exp Immunol 1984;58:183–192.
14 Ishii Y, Kon S, Takei T, *et al.* Four distinct antigen systems on human thymus and T cells defined by monoclonal antibodies: immunohistological and immunochemical studies. Clin Exp Immunol 1983;53: 31–40.
15 Fujimoto J, Ishimoto K, Kiyokawa N, *et al.* Immunocytological and immunochemical analysis on the common acute lymphoblastic leukemia antigen (CALLA): evidence that CALLA on ALL cells and granulocytes are structurally related. Hybridoma 1988;7:227–236.
16 Ishii E, Fujimoto J, Tanaka S, *et al.* Immunohistochemical analysis on normal nephorogenesis and Wilms' tumor using monoclonal antibodies reactive with lymphohaematopoietic antigens. Virchows Arch A Pathol Anat Histopathol 1987;411:315–322.
17 Neth O, Seidemann K, Jansen P, *et al.* Precursor B-cell lymphoblastic lymphoma in childhood and adolescence: clinical features, treatment, and results in trials NHL-BFM 86 and 90. Med Pediatr Oncol 2000;35: 20–27.
18 Kavan P, Kabickova E, Gajdos P, *et al.* Treatment of children and adolescents with non-Hodgkin's lymphoma (results based on the NHL Berlin–Frankfurt–Munster 90 protocols). Cas Lek Cesk 1999;138:40–46.
19 Kung PC, Long JC, McCaffrey RP, *et al.* Terminal deoxynucleotidyl transferase in the diagnosis of leukemia and malignant lymphoma. Am J Pathol 1978;64:788–794.
20 Mertelsmann R, Moore MA, Clarkson B. Methods and clinical relevance of terminal deoxynucleotidyl transferase determination in leukemic cells. Haematol Blood Transfus 1981;26:68–72.
21 Orazi A, Cattoretti G, Jphn K, *et al.* Terminal deoxynucleotidyl transferase staining of malignant lymphomas in paraffin sections. Mod Pathol 1994;7: 582–586.
22 Kaleem Z, Crawford E, Pathan MH, *et al.* Flow cytometric analysis of acute leukemias. Diagnostic utility and critical analysis of data. Arch Pathol Lab Med 2003;127:42–48.
23 Hsiao CH, Su IJ. Primary cutaneous pre-B lymphoblastic lymphoma immunohistologically mimics Ewing sarcoma/primitive neuroectodermal tumor. J Formos Med Assoc 2003;102:193–197.

Microbiol. Immunol., 48(5), 377–387, 2004

Characterization of a Shiga-Toxin 1-Resistant Stock of Vero Cells

Takaomi Sekino[1,*], Nobutaka Kiyokawa[*,1], Tomoko Taguchi[1], Hisami Takenouchi[1], Jun Matsui[1], Wei-Ran Tang[1], Toyo Suzuki[1], Hideki Nakajima[1], Masahiro Saito[1], Kazuhiro Ohmi[1], Yohko U. Katagiri[1], Hajime Okita[1], Hiroshi Nakao[2], Tae Takeda[3,†], and Junichiro Fujimoto[1]

[1]*Department of Developmental Biology, National Research Institute for Child Health and Development, Setagaya-ku, Tokyo 154–8567, Japan,* [2]*Faculty of Pharmaceutical Sciences, Okayama University, Okayama, Okayama 700–8530, Japan, and* [3]*Department of Infectious Diseases Research, National Children's Medical Research Center, Setagaya-ku, Tokyo 154–8567, Japan*

Received November 5, 2003; in revised form, January 26, 2004. Accepted February 16, 2004

Abstract: **Shiga toxins (Stxs, also referred to as verotoxins) were first described as a novel cytotoxic activity against Vero cells. In this study, we report the characterization of an Stx1-resistant (R-) stock of Vero cells. (1) When the susceptibility of R-Vero cells to Stx1 cytotoxicity was compared to that of Stx1-sensitive (S-) Vero cells by methylthiazolyldiphenyl-tetrazolium bromide (MTT) assay, cell viability after 48-hr exposure to 10 pg/ml of Stx1 was greater than 80% and less than 15%, respectively. (2) Although both a binding assay of fluorescence-labeled Stx1 and lipid analysis indicated considerable expression of Gb3Cer, a functional receptor for Stxs, in both Vero cells, anti-Gb3Cer monoclonal antibodies capable of binding to S-Vero cells failed to effectively label R-Vero cells, suggesting a conformational difference in the Gb3Cer expressed on R-Vero cells. (3) The lipid analysis also showed that the R-Vero cells contained significant amounts of Gb4Cer. In addition, introduction of exogenous Gb4Cer into S-Vero cells slightly inhibited Stx1 cytotoxicity, suggesting some correlation between glycosphingolipid composition and Stx1 resistance. (4) Both butyrate treatment and serum depression eliminated the Stx1 resistance of R-Vero cells. (5) The results of the analysis by confocal microscopy suggest a difference in intracellular transport of Stx1 between R-Vero and S-Vero cells. Further study of R-Vero cells may provide a model of Stx1 resistance via distinct intracellular transport of Stx1.**

Key words: **Shiga toxin, Vero cells, Toxin-resistant, Globotriaocyl ceramide**

Shiga toxin (Stx) is a family of protein toxins produced by Stx-producing strains of *Escherichia coli* (STEC), such as O157:H7, and it has been postulated to be the major cause of the development of serious complications associated with STEC infection, including hemolytic uremic syndrome (7, 29). Stx consists of two major types, Stx1 and Stx2. Stx1 differs from the Stx of *Shigella dysenteriae* type1 by a single amino acid in the A-subunit (15), while the amino acids of Stx2 are approximately 55% homologous with those of Stx1 (19).

All of these toxins are complexes of proteins consisting of two components, an A-subunit monomer and a B-subunit pentamer (17). The A subunit is a 30-kDa cytotoxic chain that possesses RNA *N*-glycohydrolase activity and cleaves a specific adenine residue on the 28S ribosomal RNA, resulting in inhibition of protein synthesis (17). By contrast, the 7-kDa B-subunit possesses the ability to bind with high affinity to the terminal digalactose of globotriaosyl ceramide (Gb3Cer), the functional receptor for Stx found on the specific types of the cells (17). Although Stx cytotoxicity is thought to

Address correspondence to Dr. Nobutaka Kiyokawa, Department of Developmental Biology, National Research Institute for Child Health and Development, 3–35–31 Taishido, Setagaya-ku, Tokyo 154–8567, Japan. Fax: +81–3–3487–9669. E-mail address: nkiyokawa@nch.go.jp

*Present address: Department of Pediatrics, University of Yamaguchi School of Medicine, Yamaguchi, Yamaguchi, Japan.

†Tae Takeda, M.D. & Ph. D. Died on May 15, 2001.

Abbreviations: Ab, antibody; FITC, fluorescein isothiocyanate; Gb3Cer, globotriaosyl ceramide; Gb4Cer, globotetraosyl ceramide; MTT, methylthiazolyldiphenyl-tetrazolium bromide; PBS, phosphate buffered saline; R-, resistant; S-, sensitive; STEC, Shiga-toxin-producing strains of *Escherichia coli*; Stx, Shiga toxin.

arise from the A-subunit that mediates the inhibition of protein synthesis, Stx must first bind to Gb3Cer on the target cell surface via its B-subunit, undergo endocytosis and be translocated to the cytosol to exert its cytotoxic effect.

Upon binding to Gb3Cer on the cell surface, Stx is aggregated into clathrine-coated pits and endocytosed (17, 32). After internalization, a portion of the internalized Stx molecules is delivered to the trans-Golgi network. Retrograde transport then carries the Stx molecules through the Golgi cisterns all the way to the endoplasmic reticulum, where the translocation of the A-subunit to the cytosol occurs (3, 17, 32). There, the Stx A-subunit displays its cytotoxicity by initiating RNA cleavage, thereby inhibiting protein synthesis. However, the existence of an alternate route of toxin transport to the lysosomes for degradation has also been reported (32).

Thus, the cytotoxicity of Stx is highly selective toward specific types of cells that express Gb3Cer, and, for example, it is widely believed that endothelial cells that express Gb3Cer are the main targets of Stx cytotoxicity in STEC infection (10, 23, 24, 36). In addition, renal tubular epithelial cells (5, 8, 12), mesangial cells (33, 40), macrophages/monocytes (37, 39), and neuronal cells (20, 30), all of which express Gb3Cer, have also been found to be directly affected by Stx. In addition to normal cells, a number of cell lines have been reported to be sensitive to Stx cytotoxicity. For example, the reason Stx is also called verotoxin is that it was first discovered as a novel cytotoxin toward Vero cells, which were derived from the kidneys of African green monkeys and express Gb3Cer (14). Burkitt's cell lines, such as Daudi (18) and renal-carcinoma-derived ACHN cells (34, 35), have also been reported to express Gb3Cer and to be highly sensitive to Stx.

However, several previous reports have revealed the existence of subclones of these cell lines that are resistant to Stx cytotoxicity. For example, Kongmuang et al. reported isolation of Stx-resistant Vero cells by treating them with nitrosoguanidine (13). Pudymaitis et al. also reported isolation of subclones of Daudi and Vero cells both of which are resistant for Stx (28). In each case, the mechanism of the toxin resistance has been explained by the lack of the Stx receptor Gb3Cer and the consequent inability of Stx to bind to the cells. In this paper, we report an Stx1-resistant stock of Vero cells that express Gb3Cer. Although Stx1 surely binds and is incorporated into the cells, significant resistance to cell death was observed in this stock. Further investigation the mechanism of resistance of the cells to Stx1 should help better understand the molecular mechanism of the cytotoxic action of Stx1 and provide a new approach to the prevention and treatment of Stx1 cytotoxicity during STEC infection.

Materials and Methods

Materials and cell culture. In this study, two different stocks of Vero cells, the one stored in the Department of Infectious Diseases Research, National Children's Medical Research Center, and the stock newly distributed by the Institute for Fermentation (Osaka, Japan), were used. An epidermoid carcinoma cell line A431 was obtained from the Japanese Cancer Research Resources Bank (Tokyo). Cells were cultured at 37 C in Dulbecco's Modified Eagle Medium supplemented with 10% fetal calf serum under a humidified 5% CO_2 atmosphere.

Stx1 was prepared as described previously (22) and distributed by Seikagaku Co. (Tokyo). The pentamer recombinant B-subunit of Stx1 was prepared as described previously (21). Conjugation of Stx1 with Alexa Fluor™488 (Molecular Probes, Inc., Eugene, Ore., U.S.A.) was performed according to the manufacturer's protocol. The rat monoclonal antibody (Ab) against Gb3Cer (38.13) was purchased from Beckman/Coulter (Westbrook, Mass., U.S.A.). The mouse monoclonal Ab against Gb3Cer (1A4) was a generous gift of Dr. S. Hakomori of the University of Washington, Seattle, Wash., U.S.A., and Otsuka Assay Laboratories (Kawauchi-cho, Tokushima, Japan). Mouse monoclonal Ab against the Stx1 B-subunit (13C4) was distributed by American Type Culture Collection (ATCC, Rockville, Md., U.S.A.). Secondary Abs, including fluorescein-conjugated Abs and enzyme-conjugated Abs, were purchased from Molecular Probes and Jackson ImmunoResearch Laboratories, Inc. (West Grove, Pa., U.S.A.), respectively. Purified Gb3Cer, globotetraosyl ceramide (Gb4Cer), sodium butyrate, and all other chemical reagents were obtained from Sigma-Aldrich Fine Chemicals (St. Louis, Mo., U.S.A.), unless otherwise indicated.

For cell culture, 2.5–20 mM stocks of Gb4Cer were prepared by dissolving in dimethyl sulfoxide and were added to the culture medium at a 1:1,000 dilution ratio to make the final concentration of 2.5–20 mM. Similarly, 1 M stock of sodium butyrate in phosphate buffered saline (PBS) was added to the culture medium at a 1:1,000 dilution ratio to make the final concentration of 1 mM. For serum starvation, cells were cultured under the condition of 1% FCS for 48 hr prior to the experiments.

Cell viability assay. Vero cells were plated on 96-well plates (Corning, Inc., Corning, N.Y., U.S.A.) at 1×10^4 cells in 100 µl of medium per well to achieve approximately three quarters confluence and they were then allowed to settle by overnight cultivation. After incu-

bation with different concentrations of Stx1 as indicated in each figure for 48 hr, viable cell counts were estimated by a modified methylthiazolyldiphenyl-tetrazolium bromide (MTT) assay as described previously (4), and they were expressed as a percentage of the untreated cell count. Experiments were performed in triplicate, and the means+SD of the values are shown in the figure.

Flow cytometric analysis and detection of apoptosis. For flow cytometry, cell suspensions of Vero cells were produced by treating the cells with trypsin-EDTA and pipetting. Fluorescent immunocytostaining was performed as described previously (2). To detect binding with holotoxin and the B-subunit of Stx1, one million cells in suspension were incubated with 100 ng/ml of Alexa Fluor™488-labeled holotoxin and the B-subunit of Stx1 in 100 μl of medium, respectively, for 30 min at 4 C. After intensive washing with PBS, cells were analyzed by flow cytometry (EPICS-XL, Coulter) as described previously (12, 34). Apoptosis was detected by staining with fluorescein isothiocyanate (FITC)-labeled annexin V for 15 min at room temperature by using an MEBCYTOR®-Apoptosis Kit (Medical & Biological Laboratories Co., Ltd., Nagoya, Aichi, Japan) according to the manufacturer's protocol.

Lipid analysis and TLC-blotting. The lipids were extracted from 1×10^7 of Vero cells with chloroform/methanol (2:1, v/v). The entire lipids were separated on a high performance thin-layer chromatography (TLC) plate (Merck, Darmstadt, Germany) in a chloroform/methanol/0.2% $CaCl_2$ (60:35:8, v/v/v) solvent system and visualized by spraying orcinol/H_2SO_4, as described previously (9). As a control, 1 μg each of the standard lipids of LacCer, Gb3Cer, and Gb4Cer were separated on a TLC plate simultaneously and the position of each lipid was indicated in the figure.

TLC-blotting for the detection of Stx1 binding was performed as described previously (9). Briefly, entire lipids extracted from 1×10^6 of Vero cells were separated on a TLC plate as described above and were transferred to a PVDF membrane, followed by blocking with 5% skimmed milk in PBS. After incubation with Stx1 B-subunit at 100 ng/ml for 30 min at room temperature, the membrane was washed with PBS containing 0.025% Tween 20 (Sigma), incubated with anti-Stx1 B-subunit Ab at 1 μg/ml for 30 min at room temperature, and washed again. After further incubation with peroxidase-conjugated secondary Ab at 1 μg/ml for 30 min at room temperature and the following final washing, the membrane was visualized with enhanced-chemiluminescence (ECL Westernblotting system, Amersham Pharmacia Biotech, U.K. Ltd., Buckinghamshire, U.K.). The results obtained from a 1-min exposure of the ECL-treated membrane to film are presented. TLC-blotting for the detection of Gb3Cer was performed using anti-Gb3Cer Abs in essentially the same manner as described above with an exception of the absence of preincubation with Stx1 B-subunit.

Confocal microscopic analysis of Stx1 incorporated in to the cells. For immunohistochemical detection of incorporated Stx1, 5×10^5 cells in 2 ml of medium were plated on collagen-coated cover slips (Iwaki Glass, Inc., Tokyo) placed in a 35 mm culture dish and grown overnight to achieve approximately a half confluence. At the end of the culture period, Stx1 was bound to the cells by incubation at 100 ng/ml in 1 ml of medium for 30 min at 4 C and then washed intensively with ice-cold PBS to remove the excess toxin. To allow incorporation of the toxin, cells were incubated for 4 hr in a fresh medium with shifts in temperature from 4 C to 37 C. The cover slips were then washed with PBS and fixed with 100% acetone for 15 min at 4 C, followed by incubation with anti-Stx1 Ab 13C4 at 10 μg/ml in 1 ml of medium for 60 min at room temperature and intensive washing with PBS. After incubation with Alexa Fluor™488-conjugated secondary Abs (Molecular Probes) at 10 μg/ml for 30 min and following nuclear counter staining with DAPI (200 ng/ml) for 15 min, the cover slips were washed and mounted on slide glasses using PermaFluor™ Aqueous mounting medium (Thermo Shandon, Pittsburgh, Pa., U.S.A.) and examined by confocal microscope.

For the colocalization analysis of Stx1 with lysosomal marker in R-Vero cells, a 35 mm polylysine-coated glass bottom dish (Matsunami Glass Ind., Ltd., Tokyo) and Alexa Fluor™488-conjugated Stx1 were used and the toxins were incorporated in a similar procedure as described above while the lysosome-selective probe LysoTracker RED DND-99 (final concentration of 50 nM, Molecular Probes) was added to the medium 1 hr after the temperature shift to 37 C. At the end of incubation, dishes were intensively washed with PBS and cells were mounted using aqueous mounting medium and examined by confocal microscope.

Confocal laser scanning was performed using an FV500 confocal laser scanning microscope (Olympus, Tokyo). Simultaneous multi-fluorescence acquisitions were performed using the 351-nm, 488-nm, and 543-nm laser lines to excite DAPI, Alexa Fluor™488, and RED DND-99, respectively, using a water-immersion objective (×40, NA1.7). Fluorescent images were selected using appropriate multi-fluorescence dichroic mirrors and band pass filters using the sequential acquisition mode.

Results

Identification of the Shiga-Toxin 1-Resistant Stock of Vero Cells

Vero cells have been reported to be highly sensitive to Stx cytotoxicity (14), and the Vero cells stored in our laboratory {designated as sensitive (S-) Vero in this paper for convenience} display high sensitivity to Stx1, and their cell viability is markedly reduced in a time and dose-dependent manner after Stx1 treatment. As shown in Fig. 1A, after treatment for 48 hr, 10 pg/ml of Stx1 induced about an 80% reduction in the number of cells as assessed by MTT assay. Previous reports, including our own, have indicated that apoptosis is involved in the process of Stx-mediated cell death (6, 18, 34, 38). As shown in Fig. 1B, flow cytometric analysis revealed that 62.4% of S-Vero cells bound to annexin V after a 48-hr treatment with 10 pg/ml of Stx1, suggesting a significant induction of apoptosis in S-Vero cells.

In the process of comparing the Stx1 sensitivity of different stocks of Vero cells, however, we found that the stock of Vero cells distributed by the Institute for Fermentation {designated resistant (R-) Vero in this paper for convenience} exhibit low sensitivity to Stx1. As shown in Fig. 1A, after treatment for 48 hr, 10 pg/ml of Stx1 induced only about a 20% reduction in the number of cells, as assessed by MTT assay. Even at a higher concentration, 100 pg/ml, approximately 75% of the cells were still viable (Fig. 1A). In parallel, flow cytometric analysis revealed that only 22.9% of the R-Vero cells bound to annexin V after 48-hr treatment with 10 pg/ml of Stx1 (Fig. 1B). The data indicate reduced sensitivity of R-Vero cells to Stx1. We also tested Stx2 cytotoxicity against both S- and R-Vero cells and essentially observed results similar as to those for Stx1 (data not shown).

Distinct Gb3Cer Expression in the Shiga-Toxin 1-Resistant Stock of Vero Cells

Next, we measured the level of expression of Gb3Cer in S- and R-Vero cells by several different methods. When the expression level of Gb3Cer was measured by flow cytometry with anti-Gb3Cer 38.13 mAbs, the S-Vero cells showed a heterogeneous staining pattern, and their fluorescence intensity ranged from very weak to strong (Fig. 2). By contrast, when R-Vero cells were similarly tested, they showed only weak staining with 38.13 mAb (Fig. 2). When we tested another anti-Gb3Cer mAb, 1A4, we observed identical results (Fig. 2). Curiously, however, when binding of FITC-labeled Stx1 was examined by flow cytometry, the results showed significant binding of Stx1 by R-Vero cells (Fig. 2). As shown in Fig. 2, some of the R-Vero cells showed stronger fluorescence intensity after incubation with FITC-Stx1 than the S-Vero cells. We obtained similar results when we tested binding of the FITC-labeled B-subunit of Stx1 (Fig. 2).

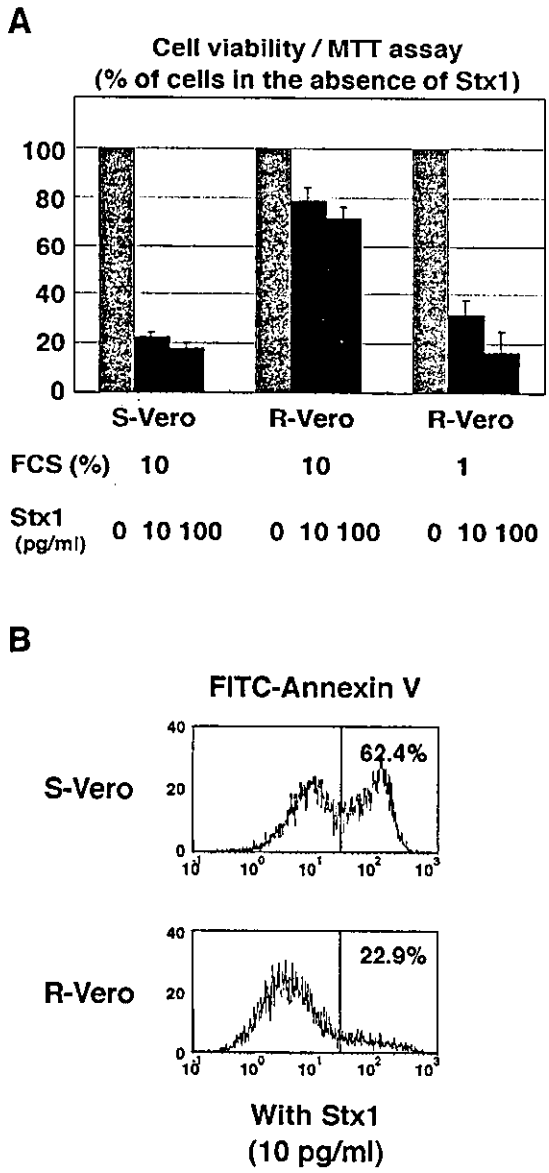

Fig. 1. Susceptibility of different stocks of Vero cells to Shiga toxin 1 (Stx1) cytotoxicity. A: After 48 hr of incubation with different concentrations of Stx1, viable cell counts of sensitive (S-) and resistant (R-) Vero cells were estimated by MTT assay. Two different concentrations of FCS, 10% and 1%, were tested on R-Vero cells as described in "Materials and Methods." B: Vero cells treated in the same manner as in A. After incubation, apoptotic cells were detected by annexin V-binding assay using flow cytometry. The resulting histograms show the percentages of annexin V-bound cells. X-axis, fluorescence intensity; Y-axis, relative cell number.

The above results may seem to suggest that R-Vero

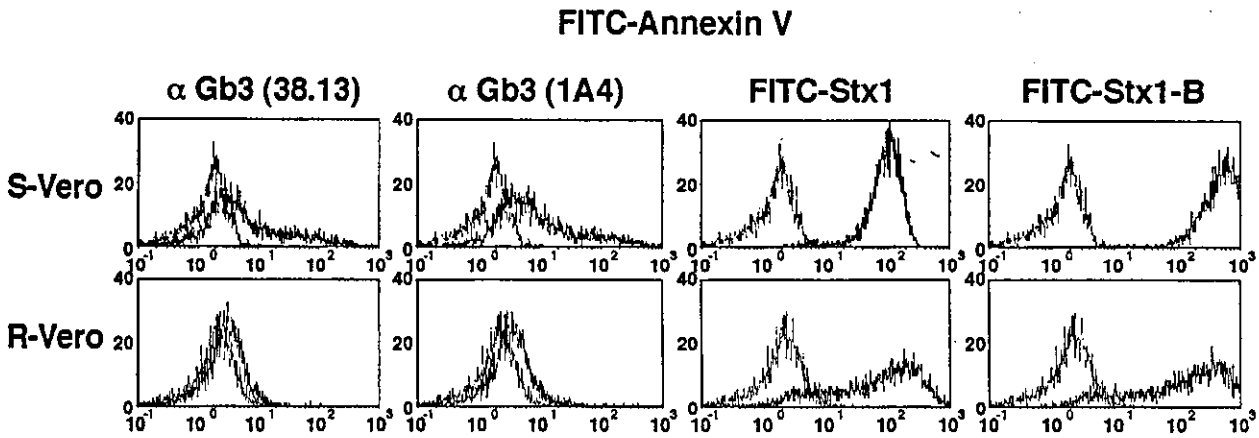

Fig. 2. Expression of globotriaosyl ceramide (Gb3Cer) and cell surface binding of Shiga toxin 1 (Stx1). Cell suspensions obtained from sensitive (S-) (upper panel) and resistant (R-) Vero cells (lower panel) were incubated with FITC-labeled anti-Gb3Cer monoclonal antibodies or Alexa Fluor™488-conjugated holotoxin and the B-subunit of Stx1, and analyzed by flow cytometry. The histogram obtained has been superimposed on that of the negative control. X-axis, fluorescence intensity; Y-axis, relative cell number.

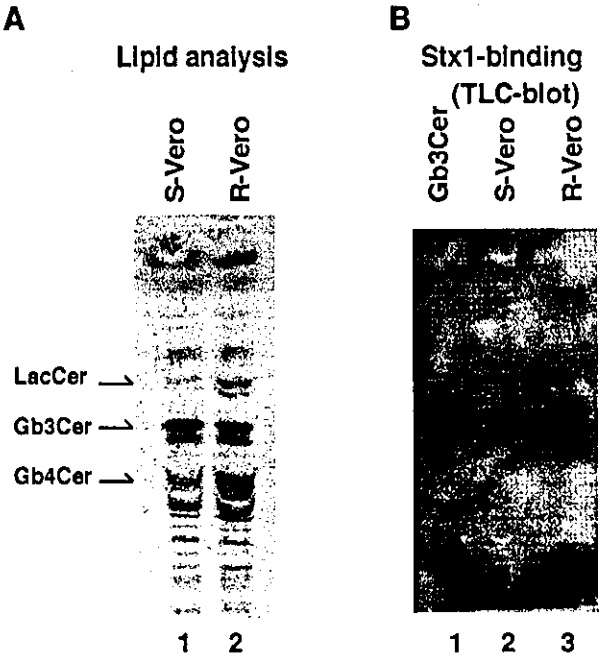

Fig. 3. Lipid analysis of Vero crlls. A: The lipids of sensitive (S-) (left lane) and resistant (R-) Vero cells (right lane) were analyzed as described in "Materials and Methods." B: Binding of Shiga toxin 1 (Stx1) to lipids extracted from S- (mid lane) and R-Vero cells (right lane) was assessed by TLC-blotting. As a control, purified globotriaosyl ceramide was tested at the same time (left lane).

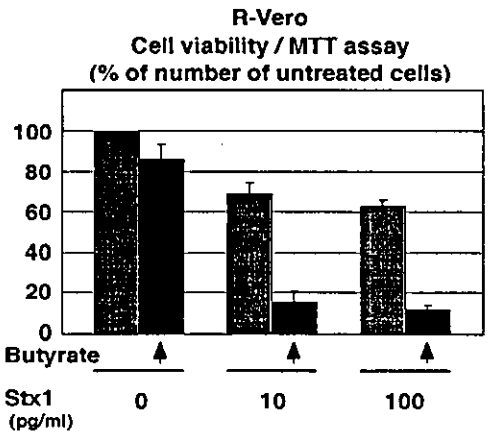

Fig. 4. Effect of sodium butyrate on the Shiga toxin 1 (Stx1) sensitivity of Vero cells. Resistant (R-) Vero cells pre-incubated and not incubated with 1 mM of sodium butyrate for 24 hr were exposed to Stx1for 48 hr. The number of viable cells was determined by MTT assay as in Fig. 1A.

cells express other receptor(s) for Stx1 and may not express Gb3Cer. However, as shown in Fig. 3A, lipid analysis revealed that almost the same amount of Gb3Cer was expressed by the R-Vero cells as by the S-Vero cells. In addition, TLC-blotting analysis revealed that Stx1 only binds Gb3Cer and no other components of the lipids extracted from either R- or S-Vero cells (Fig. 3B). Moreover, both anti-Gb3Cer Abs could recognize Gb3Cer extracted from R-Vero cells similary as that from S-Vero cells in TLC-blotting (data not shown). Therefore, it seems most likely that R-Vero cells express a considerable amount of Gb3Cer on the cell surface, and thus bind with Stx1, but that the anti-Gb3Cer Ab binding site in Gb3Cer is conformationally masked by an unknown modification specifically present in the cell membrane of R-Vero cells. It is noteworthy that the amounts of LacCer and Gb4Cer are higher in R-Vero cells than in S-Vero cells (Fig. 3A).

Effect of Butyrate, Serum Depletion, and Exogenous Gb4Cer on Stx1 Cytotoxicity against Vero Cells

Since treatment with butyrate has been reported to

enhance cell sensitivity to Stx cytotoxicity (31), next, we investigated whether treatment with butyrate affects the cytotoxic effect of Stx1 on R-Vero cells. Interestingly, when 1 mM sodium butyrate was added to the medium 24 hr prior to the challenge of the toxin, the sensitivity of R-Vero cells to Stx1 cytotoxicity significantly increased, and 10 pg/ml of Stx1 induced a more than 90% reduction in the number of cells after 48 hr of incubation, as assessed by MTT assay (Fig. 4A).

We also investigated whether serum depletion affects the cytotoxic effect of Stx1 on R-Vero cells. When R-Vero cells cultured under low serum conditions of 1% FCS for 48 hr were treated with Stx1, Stx1 cytotoxicity was significantly enhanced, and more than a 60% and 80% reduction in the number of cells was observed by MTT assay after 48-hr incubation with 10 and 100 pg/ml Stx1, respectively (Fig. 1A).

In parallel, we measured the Gb3Cer expression level in serum depleted R-Vero cells by flow cytometry and compared it with that in R-Vero cells under regular culture conditions with 10% FCS that was indicated in Fig. 2. However, no significant change was observed in both staining patterns with anti-Gb3Cer Abs and binding of Stx1 (data not shown), suggesting that serum depletion does not affect the expression level of Gb3Cer in R-Vero cells.

Since we observed an increased level of Gb4Cer in R-Vero cells, next, we investigated whether an addition of exogenous Gb4Cer would affect Stx1 cytotoxicity against S-Vero cells. As shown in Fig. 5, when S-Vero cells were incubated with culture medium containing 10 μM of Gb4Cer for 24 hr prior to Stx1 treatment, Stx1 cytotoxicity assessed by annexin V-binding assay was slightly, but clearly, decreased. In an attempt to see the more significant inhibition of Stx1 cytotoxicity mediated by Gb4Cer, we tested different experimental conditions. As shown in Fig. 5B, the inhibitory effect tended to be dependent on the Gb4Cer dose. However, increasing amounts of Gb4Cer did not result in significant enhancement of apoptosis inhibition even if the amount of Stx1 was decreased. The data indicate that the effect of exogenous Gb4Cer on Stx1 cytotoxicity is limited.

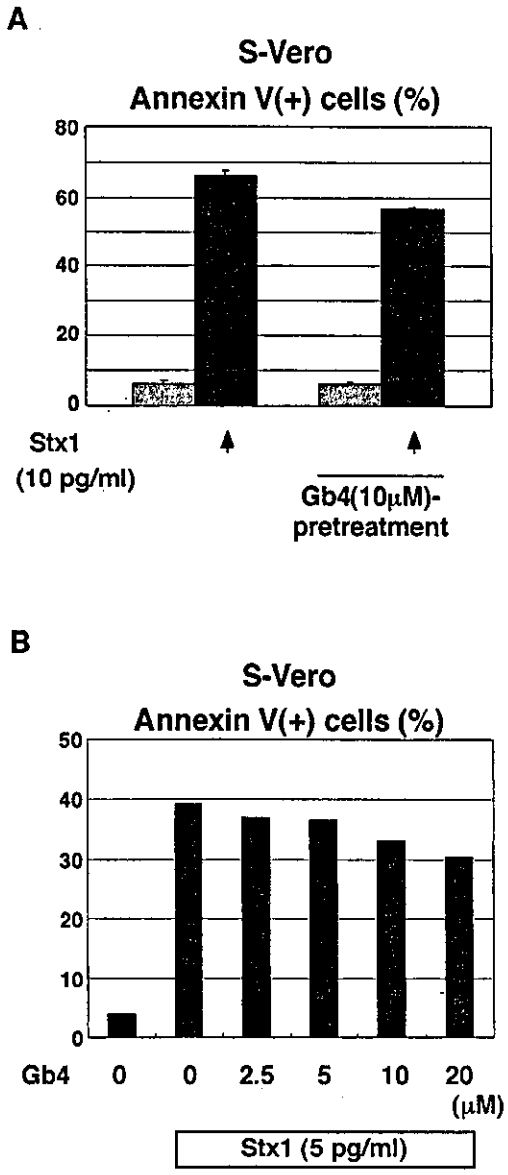

Fig. 5. Effect of endogenous Gb4Cer on the Shiga toxin 1 (Stx1) sensitivity of Vero cells. A: Sensitive (S-) Vero cells pre-incubated and not incubated with 10 μM Gb4Cer for 24 hr were exposed to Stx1 for 48 hr. FITC-annexin V binding was assessed as in Fig. 1B. Experiments were performed in triplicate, and the means+SD of the values are indicated. B: S-Vero cells pre-incubated and not incubated with Gb4Cer at the different concentrations as indicated in the figure for 24 hr were exposed to 5 pg/ml of Stx1 for 48 hr. FITC-annexin V binding was assessed as in A.

Fig. 6. Localization of incorporated Shiga toxin 1 (Stx1) in sensitive (S-) and resistant (R-) Vero cells. A: Stx1 incorporated in S- and R-Vero cells were stained with the combination of anti-Stx1 antibody 13C4 and Alexa Fluor™488-conjugated secondary antibody (green) as described in "Materials and Methods." Nuclei were counterstained with DAPI (blue). Incorporated Stx1 was visualized by confocal microscopy. The peri-nuclear localizations of Stx1 were indicated by arrows. B: Stx1 incorporated in A431 cells was detected as in A. C: The localizations of incorporated Stx1 (green) and a lysosomal marker LysoTracker RED DND-99 (red) in R-Vero cells were simultaneously examined by confocal microscopy as described in "Materials and Methods." In the bottom panel, both images were superimposed with nuclear staining (blue).

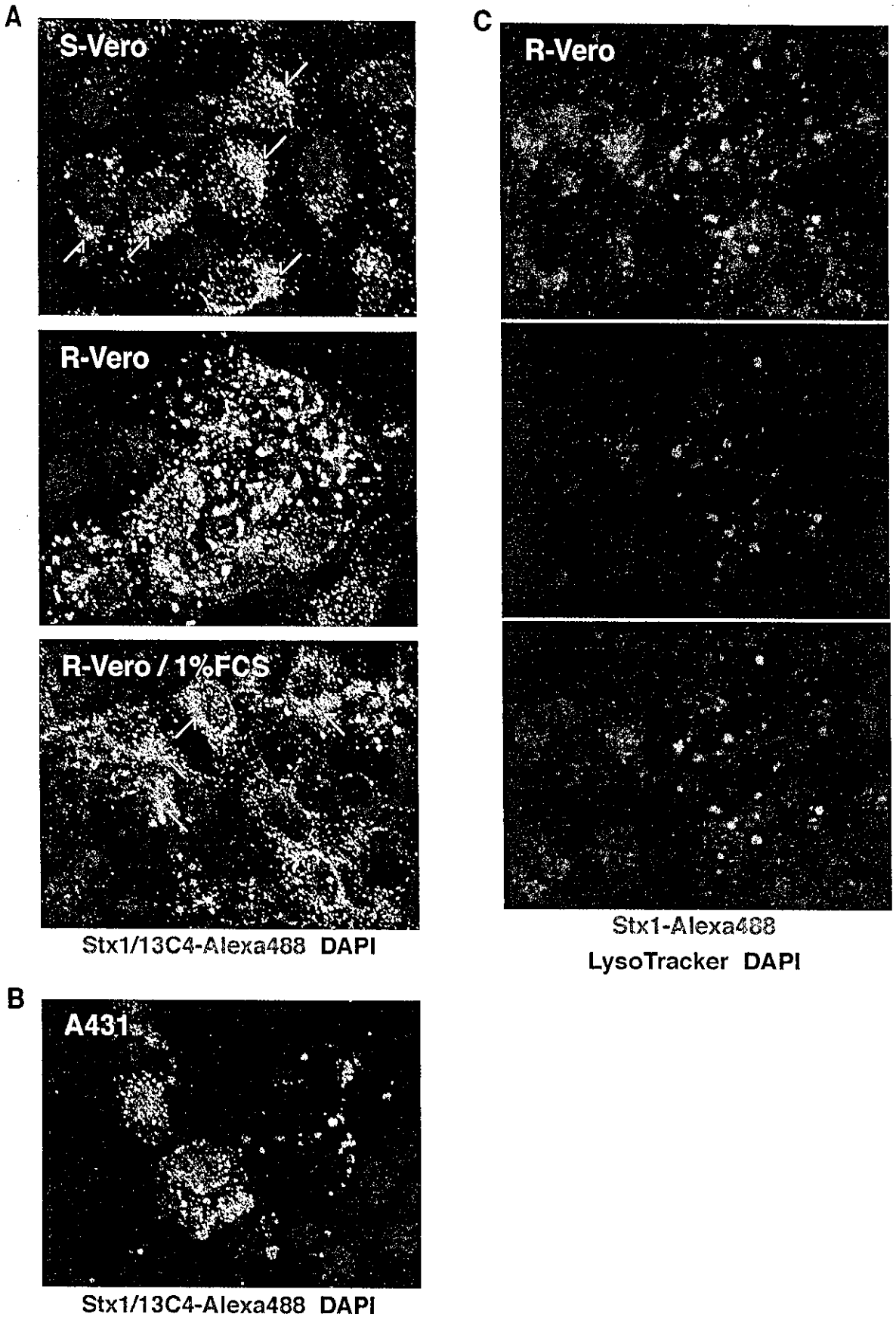
A
S-Vero
R-Vero
R-Vero / 1%FCS
Stx1/13C4-Alexa488 DAPI
B
A431
Stx1/13C4-Alexa488 DAPI
C
R-Vero
Stx1-Alexa488
LysoTracker DAPI

Fig. 6.

Different Intracellular Transport of Stx1 in S- and R-Vero Cells

Stx1 may be able to bind R-Vero cells but not be incorporated by them, with the cells escaping cell death as a result. To test this possibility, we used confocal laser scanning microscopy to determine whether fluorescein-conjugated Stx1 is incorporated by S- and R-Vero cells. As shown in Fig. 6A (upper panel), Stx1 was incorporated into the S-Vero cells and transported to the peri-nuclear area after 4 hr (pointed by arrows). Interestingly, Stx1 was also incorporated significantly by the R-Vero cells, but the localization of the toxin was different from its localization in S-Vero cells. As shown in Fig. 6A (mid panel), the Stx1 incorporated into the R-Vero cells exhibited a granular pattern within the cytoplasm. We also examined the effect of serum depletion on the intracellular transport of Stx1 in R-Vero cells. As shown in Fig. 6A (lower panel), when Stx1 was incorporated in R-Vero cells precultured under the condition of 1% FCS for 48 hr, an increase in the number of the cells in which Stx1 localized in peri-nuclear area was observed (pointed by arrows). The date suggests that the serum depletion affects the intracellular transport of Stx1 in R-Vero cells.

As we mentioned above, the existence of an alternate route of toxin transport to the lysosomes for degradation in some cells, such as A431 cells, has been reported (32). As shown in Fig. 6B, when we examined the localization of Stx1 in A431 cells, the incorporated toxin exhibited a granular pattern within the cytoplasm similar to that in R-Vero cells. Therefore, we examined whether incorporated Stx1 in R-Vero cells colocalize with the lysosomal marker. When the intracellular localization of Alexa Fluor™488-conjugated Stx1 and the lysosome-selective probe LysoTracker RED DND-99 in R-Vero cells were simultaneously examined, the colocalization of these molecules was observed (Fig. 6C). The data suggest that a large propotion of the Stx1 incorporated in R-Vero cells is transported to lysosomes under the regular culture condition with 10% FCS.

Discussion

In this study, we demonstrated the existence of an Stx1-resistant stock of Vero cells. Although Stx1-resistant cell clones of Vero cells have been reported by other groups, the mechanism of the Stx1 resistance in our R-Vero cells and others seems to be different. For example, Kongmuang et al. reported Stx-resistant Vero cells that were isolated by treating the cells with nitrosoguanidine and had lost their toxin-binding capacity as assessed by immunofluorescent analysis (13). Pudymaitis et al. reported a Stx-resistant Vero cell clone that was isolated by its ability to grow in the presence of Stx2 at a concentration of approximately 7 ng/ml and was found to be deficient in Gb3Cer (28). Therefore, the main mechanism of the Stx resistance in the previous examples of Stx-resistant Vero cell clones was a lack of toxin-binding capacity, whereas as shown in this report, our Stx1-resistant Vero cells express an amount of Gb3Cer comparable to that of Stx1-sensitive Vero cells and possess considerable toxin-binding capacity. Indeed, we confirmed significant toxin incorporation into the R-Vero cells by confocal microscopic study (Fig. 6).

Interestingly, Sandvig et al. demonstrated another mechanism of Stx resistance (31). They reported that cell line A431 derived from epidermoid carcinoma, which expresses Gb3Cer and has toxin-binding capacity, is completely resistant to Stx. However, A431 cells acquire Stx sensitivity when cultured in the presence of butyrate, and the mechanism of their distinct sensitivity to Stx cytotoxicity is explained by an alteration in the transport route of Stx after receptor-mediated endocytosis. It has been well documented that retrograde transport of Stx into cytoplasm, where Stx cleaves RNA, is required for expression of cytotoxicity by Stx (17, 31). Under regular culture conditions, most of the toxins in A431 cells resistant to Stx are transported to the lysosomes and degraded, thereby destroying its cytotoxicity. In butyrate-treated A431 cells, however, internalized toxins are routed to the cytoplasm through the Golgi network and endoplasmic reticulum, and thus they exhibited significant sensitivity to Stx cytotoxicity (31). Although further investigations are needed, the mechanism of the Stx1 resistance that we observed in R-Vero cells may be the same as in A431 cells. Our finding of different localizations of the Stx1 incorporated into R- and S-Vero cells, of Stx1 colocalization with the lysosomal marker in R-Vero cells, and of butyrate-mediated sensitization of R-Vero cells to Stx1 should support this notion.

It is noteworthy that Stx1 bound to the Gb3Cer expressed on the cell surface of the R-Vero cells, whereas anti-Gb3Cer monoclonal Ab showed less ability to bind to Gb3Cer. Previously, Lingwood and co-worker demonstrated that the fatty acid composition of Gb3Cer influences its ability to bind to ligands. For example, Gb3Cer containing fatty acid species shorter than C14 were found to be ineffective as receptors for Stx in a phosphoplipid matrix, whereas when fatty acids longer than C20 were used, the species were effectively recognized by Stx but were no longer substrates for galactose oxidase (26), indicating that different epitopes required by these two different ligands (Stx and galactose oxidase) are differentially expressed on different Gb3Cer fatty acid homologues (1, 41). Considering their reports,

it seems to be a plausible explanation that the difference in fatty acid composition of Gb3Cer between R- and S-Vero cells may exist and affect the recognition of Gb3Cer by anti-Gb3Cer monoclonal Abs, but not by Stx1. However, they also reported that the fatty-acid length influences the mobility of Gb3Cer in TLC (11). Since no significant difference was observed in the mobility between Gb3Cer of R-Vero and that of S-Vero in our TLC result (Fig. 3), fatty-acid lengths of both Gb3Cer are not significantly different. Therefore, the failure of the recognition of Gb3Cer expressed on R-Vero cells by the anti-Gb3Cer monoclonal Abs may not be explained by the difference in fatty acid composition. In addition, we also observed that anti-Gb3Cer antibodies could recognize Gb3Cer of R-Vero similar to that of S-Vero cells in the TLC-blot (data not shown). Although the precise reason is unknown, Gb3Cer expressed R-Vero cells are not compositionally different from that of S-Vero cells, but presented differently on the cell surface and the anti-Gb3Cer Ab binding site in Gb3Cer is conformationally masked by an unknown modification specifically present in the cell membrane of R-Vero cells.

We also observed a difference in lipid composition between R- and S-Vero cells. The amounts of both LacCer and Gb4Cer were higher in R-Vero cells than in S-Vero cells, but the amount of Gb3Cer was unchanged (Fig. 3A). Furthermore, as we showed in this study, addition of exogenous Gb4Cer reduced the Stx1 sensitivity of S-Vero cells. It was reported that purified gangliosides exogenously added to the culture medium bind and are stably incorporated in cultured cells (25). In addition, the incorporated exogenous gangliosides are thought to function as components of cell membranes (16, 27). The evidence should support the notion that preincubation of cells with exogenous glycosphingolipids is a reasonable approach to enrich cellular glycosphingolipids. Therefore, the inhibitory effect of exogenous Gb4Cer on Stx1-induced apoptosis in S-Vero cells may be a consequence of the enrichment of Gb4Cer in the cell membrane and suggest a correlation between lipid composition and Stx1 susceptibility. Although the details are unknown, the differences in lipid composition of the cell membrane may affect Gb3Cer recognition by ligands and the sorting route of incorporated Stx1. Since we also found that serum starvation increases the susceptibility of cells to Stx1 cytotoxicity, the serum concentration of the culture medium may affect the lipid composition of the cell membrane.

In conclusion, we have reported a stock of Vero cells that has the capacity to bind Stx1 but are significantly resistant to Stx1 cytotoxicity. Additional fundamental studies are clearly necessary, but clarification of the acquisition mechanism of resistance to Stx1 cytotoxicity by these cells should allow a better understanding of the molecular basis of Stx1-mediated cell damage and open the way to improved therapeutic approaches to diseases caused by Stx1.

We thank M. Sone and S. Yamauchi for their excellent secretarial work. We thank Dr. S. Hakomori and Otsuka Assay Laboratories for donating CD77 monoclonal Ab 1A4.

This work was supported in part by Health and Labour Sciences Research Grants from the Ministry of Health, Labour and Welfare of Japan and MEXT. KAKENHI 15019129, JSPS. KAKENHI 15390133 and 15590361. This work was also supported by a grant from the Japan Health Sciences Foundation for Research on Health Sciences Focusing on Drug Innovation. Additional support was provided by a grant from Sankyo Foundation of Life Science.

References

1) DeGrandis, S., Law, H., Brunton, J., Gyles, C., and Lingwood, C.A. 1989. Globotetraosylceramide is recognized by the pig edema disease toxin. J. Biol. Chem. **264**: 12520–12525.
2) Fujimoto, J., Ishimoto, K., Kiyokawa, N., Tanaka, S., Ishii, E., and Hata, J. 1988. Immunocytological and immunochemical analysis on the common acute lymphoblastic leukemia antigen (CALLA) : evidence that CALLA on ALL cells and granulocytes are structurally related. Hybridoma **7**: 227–236.
3) Garred, O., Dubinina, E., Holm, P.K., Olsnes, S., van Deurs, B., Kozlov, J.V., and Sandvig, K. 1995. Role of processing and intracellular transport for optimal toxicity of Shiga toxin and toxin mutants. Exp. Cell Res. **218**: 39–49.
4) Hansen, M.B., Nielsen, S.E., and Berg, K. 1989. Re-examination and further development of a precise and rapid dye method for measuring cell growth/cell kill. J. Immunol. Methods **119**: 203–210.
5) Hughes, A.K., Stricklett, P.K., and Kohan, D.E. 1998. Cytotoxic effect of Shiga toxin-1 on human proximal tubule cells. Kidney Int. **54**: 426–437.
6) Inward, C.D., Williams, J., Chant, I., Crocker, J., Milford, D.V., Rose, P.E., and Taylor, C.M. 1995. Verocytotoxin-1 induces apoptosis in vero cells. J. Infect. **30**: 213–218.
7) Kaplan, B.S., Cleary, T.G., and Obrig, T.G. 1990. Recent advances in understanding the pathogenesis of the hemolytic uremic syndromes. Pediatr. Nephrol. **4**: 276–283.
8) Karpman, D., Hakansson, A., Perez, M.T., Isaksson, C., Carlemalm, E., Caprioli, A., and Svanborg, C. 1998. Apoptosis of renal cortical cells in the hemolytic-uremic syndrome: *in vivo* and *in vitro* studies. Infect. Immun. **66**: 636–644.
9) Katagiri, U.Y., Mori, T., Nakajima, H., Katagiri, C., Taguchi, T., Takeda, T., Kiyokawa, N., and Fujimoto, J. 1999. Activation of Src family kinase Yes induced by Shiga toxin binding to globotriaosyl ceramide (Gb3/CD77) in low density, detergent-insoluble microdomains. J. Biol. Chem. **274**: 35278–35282.

10) Kaye, S.A., Louise, C.B., Boyd, B., Lingwood, C.A., and Obrig, T.G. 1993. Shiga toxin-associated hemolytic uremic syndrome: interleukin-1β enhancement of Shiga toxin cytotoxicity toward human vascular endothelial cells *in vitro*. Infect. Immun. **61**: 3886–3891.
11) Kiarash, A., Boyd, B., and Lingwood, C.A. 1994. Glycosphingolipid receptor function is modified by fatty acid content. Verotoxin 1 and verotoxin 2c preferentially recognize different globotriaosyl ceramide fatty acid homologues. J. Biol. Chem. **269**: 11138–11146.
12) Kiyokawa, N., Taguchi, T., Mori, T., Uchida, H., Sato, N., Takeda, T., and Fujimoto, J. 1998. Induction of apoptosis in normal human renal tubular epithelial cells by *Escherichia coli* Shiga toxins 1 and 2. J. Infect. Dis. **178**: 178–184.
13) Kongmuang, U., Honda, T., and Miwatani, T. 1988. Isolation of Shiga toxin-resistant Vero cells and their use for easy identification of the toxin. Infect. Immun. **56**: 2491–2494.
14) Konowalchuk, J., Speirs, J.I., and Stavric, S. 1977. Vero response to a cytotoxin of *Escherichia coli*. Infect. Immun. **18**: 775–779.
15) Kozlov, Y.V., Kabishev, A.A., Lukyanov, E.V., and Bayev, A.A. 1988. The primary structure of the operons coding for *Shigella dysenteriae* toxin and temperature phage H30 shiga-like toxin. Gene **67**: 213–221.
16) Li, R., Manela, J., Kong, Y., and Ladisch, S. 2000. Cellular gangliosides promote growth factor-induced proliferation of fibroblasts. J. Biol. Chem. **275**: 34213–34223.
17) Lingwood, C.A. 1996. Role of verotoxin receptors in pathogenesis. Trends Microbiol. **4**: 147–153.
18) Mangeney, M., Lingwood, C.A., Taga, S., Caillou, B., Tursz, T., and Wiels, J. 1993. Apoptosis induced in Burkitt's lymphoma cells via Gb3/CD77, a glycolipid antigen. Cancer Res. **53**: 5314–5319.
19) Melton-Celsa, A.R., and O'Brien, A.D. 1998. *Escherichia coli* O157:H7 and other Shiga toxin-producing *E. coli* strains, p. 121–128. *In* Kaper, J.B., and O'Brien, A.D. (eds), Structure, biology, and relative toxicity of Shiga toxin family members for cells and animals, ASM Press, Washington, D.C.
20) Mizuguchi, M., Tanaka, S., Fujii, I., Tanizawa, H., Suzuki, Y., Igarashi, T., Yamanaka, T., Takeda, T., and Miwa, M. 1996. Neuronal and vascular pathology produced by verocytotoxin 2 in the rabbit central nervous system. Acta Neuropathol. (Berl.) **91**: 254–262.
21) Nakajima, H., Katagiri, Y.U., Kiyokawa, N., Taguchi, T., Suzuki, T., Sekino, T., Mimori, K., Saito, M., Nakao, H., Takeda, T., and Fujimoto, J. 2001. Single-step method for purification of Shiga toxin-1 B subunit using receptor-mediated affinity chromatography by globotriaosylceramide-conjugated octyl sepharose CL-4B. Protein Expr. Purif. **22**: 267–275.
22) Noda, M., Yutsudo, T., Nakabayashi, N., Hirayama, T., and Takeda, Y. 1987. Purification and some properties of Shiga-like toxin from *Escherichia coli* O157: H7 that is immunologically identical to Shiga toxin. Microb. Pathog. **2**: 339–349.
23) Obrig, T.G., Del-Vecchio, P.J., Brown, J.E., Moran, T.P., Rowland, B.M., Judge, T.K., and Rothman, S.W. 1988. Direct cytotoxic action of Shiga toxin on human vascular endothelial cells. Infect. Immun. **56**: 2373–2378.
24) Ohmi, K., Kiyokawa, N., Takeda, T., and Fujimoto, J. 1998. Human microvascular endothelial cells are strongly sensitive to Shiga toxins. Biochem. Biophys. Res. Commun. **251**: 137–141.
25) Olshefski, R., and Ladisch, S. 1996. Intercellular transfer of shed tumor cell gangliosides. FEBS Lett. **386**: 11–14.
26) Pellizzari, A., Pang, H., and Lingwood, C.A. 1992. Binding of verocytotoxin 1 to its receptor is influenced by differences in receptor fatty acid content. Biochemistry **31**: 1363–1370.
27) Prinetti, A., Iwabuchi, K., and Hakomori, S. 1999. Glycosphingolipid-enriched signaling domain in mouse neuroblastoma Neuro2a cells. Mechanism of ganglioside-dependent neuritogenesis. J. Biol. Chem. **274**: 20916–20924.
28) Pudymaitis, A., Armstrong, G., and Lingwood, C.A. 1991. Verotoxin-resistant cell clones are deficient in the glycolipid globotriosylceramide: differential basis of phenotype. Arch. Biochem. Biophys. **286**: 448–452.
29) Richardson, S.E., Karmali, M.A., Becker, L.E., and Smith, C.R. 1988. The histopathology of the hemolytic uremic syndrome associated with verocytotoxin-producing *Escherichia coli* infections. Hum. Pathol. **19**: 1102–1108.
30) Richardson, S.E., Rotman, T.A., Jay, V., Smith, C.R., Becker, L.E., Petric, M., Olivier, N.F., and Karmali, M.A. 1992. Experimental verocytotoxemia in rabbits. Infect. Immun. **60**: 4154–4167.
31) Sandvig, K., Garred, O., Prydz, K., Kozlov, J.V., Hansen, S.H., and van Deurs, B. 1992. Retrograde transport of endocytosed Shiga toxin to the endoplasmic reticulum. Nature **358**: 510–512.
32) Sandvig, K., and van Deurs, B. 1996. Endocytosis, intracellular transport, and cytotoxic action of Shiga toxin and ricin. Physiol. Rev. **76**: 949–966.
33) Simon, M., Cleary, T.G., Hernandez, J.D., and Abboud, H.E. 1998. Shiga toxin 1 elicits diverse biologic responses in mesangial cells. Kidney Int. **54**: 1117–1127.
34) Taguchi, T., Uchida, H., Kiyokawa, N., Mori, T., Sato, N., Horie, H., Takeda, T., and Fujimoto, J. 1998. Verotoxins induce apoptosis in human renal tubular epithelium derived cells. Kidney Int. **53**: 1681–1688.
35) Takeda, T., Dohi, S., Igarashi, T., Yamanaka, T., Yoshiya, K., and Kobayashi, N. 1993. Impairment by verotoxin of tubular function contributes to the renal damage seen in haemolytic uraemic syndrome. J. Infect. **27**: 339–341.
36) Tesh, V.L., Samuel, J.E., Perera, L.P., Sharefkin, J.B., and O'Brien, A.D. 1991. Evaluation of the role of Shiga and Shiga-like toxins in mediating direct damage to human vascular endothelial cells. J. Infect. Dis. **164**: 344–352.
37) Tesh, V.L., Ramegowda, B., and Samuel, J.E. 1994. Purified Shiga-like toxins induce expression of proinflammatory cytokines from murine peritoneal macrophages. Infect. Immun. **62**: 5085–5094.
38) Uchida, H., Kiyokawa, N., Taguchi, T., Horie, H., Fujimoto, J., and Takeda, T. 1999. Shiga toxins induce apoptosis in pulmonary epithelium derived cells. J. Infect. Dis. **180**: 1902–1911.
39) van Setten, P.A., Monnens, L.A., Verstraten, R.G., van den Heuvel, L.P., and van Hinsbergh, V.W. 1996. Effects of verocytotoxin-1 on nonadherent human monocytes: binding